2007

Feasibility of using laser induced breakdown spectrograph for coal analysis for slagging propensity prediction

Yao Shen
Lehigh University

Shen, Yao

Feasibility of Using Laser Induced Breakdown Spectrograph for Coal Analysis for Slagging…

May 2007

Feasibility of Using Laser Induced Breakdown Spectrograph for Coal Analysis for Slagging Propensity Prediction

By

Yao Shen

Presented to the Graduate and Research Committee

of

Lehigh University

in Candidacy for the Degree of

Master of Science

Department of Mechanical Engineering and Mechanics

Lehigh University

04/20/2007

This thesis is accepted and approved in partial fulfillment of the requirements for the Master of Science.

April 24, 2007

Date

Thesis Advisor

Co-Advisor

Chairperson of Department

Acknowledgments

This thesis would have not been possible without the support of many people. Many thanks to my adviser and co-adviser, Dr. Edward K. Levy and Dr. Carlos E Romero, who read my numerous revisions and helped make sense of the confusion with great patience. Also thanks to our partners in Energy Research Co. in Staten Island, NY, who offered guidance and support. And finally, thanks to my wife, parents, and numerous friends who endured this long process with me, always offering supports and love.

Contents

List of Tables

List of Figures

Abstract

Laser Induced Breakdown Spectrometry (LIBS) is a technique that uses a laser-based principle to detect the chemical components of a sample. This thesis explores the feasibility of using the LIBS technology in the chemical analysis of coal samples for the formulation of slagging potential predictors. This approach would be highly valuable in coal-fired power plants. LIBS experiments were performed on both simulated and actual coal samples. Samples were prepared and their emitted spectral signals were collected and post-processed. The following elements were detected by the LIBS system: C, H, O, and S, as well as, Si, Al, Ti, Fe, Ca, Mg, Na, and K. This study includes the development of LIBS spectral-based models for the prediction of a high-temperature slagging index and the ash fusion temperature, for application in coal-fired boilers. The slagging index was developed using artificial neural networks. The ash fusion temperature prediction index was developed using a non-linear mathematical function. It was found that that the LIBS analyses can produce coal composition results that correlate well with synthetic coal samples and some standardized coal composition analysis. Reproducibility was achieved with an error of 0.3. However, improvement in the instrumentation is needed to achieve accurate analysis for a broad range of coal samples, which can be formulated into newly developed slagging potential prediction indices that would be useful to the power industry.

Chapter 1: Introduction

The first Laser Induced Breakdown Spectrometry (LIBS) demonstrations were performed in 1962. Since then, the LIBS technique has been the topic of many research investigations and developmental efforts. Despite these efforts, the impact of LIBS physical and chemical general analysis remains limited only to a few instruments in use on a commercial base. LIBS can be used for the detection of elemental and trace composition of samples of different nature. Fundamentally, LIBS can distinct itself from other detecting technologies because it is sensitive to trace concentrations of elements. Also, relatively short sample preparation time is a great advantage of LIBS when comparing to any other methods, such as acid extraction of components.

The coal-fired power generation industry is a typical example of an industry where new material analysis technologies are in demand. Elemental coal analysis in coal-fired power plants is a key measurement needed for classification and handling of various coal types and impurities. The LIBS instrumentation would be a great fit for this industry because of its many inherent advantages in analyzing for coal composition. Many of the elements present in the coal ash, such as Ti, Al, Mg, Na, Ca and K are at low concentration levels or, in some coal ranks, considered to be trace quantities. Currently, the typical elemental analysis of coal components is most widely done by acid extraction, such as in the American Society for Testing and Material (ASTM) Ultimate Analysis (Method D3176-89) etc., for ash mineral analysis determination and other subsequent analysis. LIBS is a new technology that has the potential to become an on-line tool in

the power industry, for coal-fired power plants, which would improve the flow of information available and assist the application of strategies to improve station performance.

One particular application where LIBS can be introduced in coal-fired power plants is the in-situ and on-line detection of coal elemental and ash mineral composition for inferring the slagging/fouling propensity of different fuels. Coal-fired boilers are nowadays faced with the challenge of operating with off-design fuels, with different characteristics from the design coal. This, very often, results in high-temperature slagging and convective pass fouling problems that are, most of the time, dealt after the fact. A tool that could provide coal composition-based slagging/fouling propensity information would be very helpful to anticipate these problems in different ways. The problem fuel(s) could be rejected, blended or burned in units less slag sensitive; and the boilers subject to the problem fuels could be prepared, in terms of their operation (modifying their boiler control settings and soot-blowing practices) to mitigate the slagging/fouling effect. This thesis reports laboratory work to investigate the feasibility of using LIBS spectral information to detect the chemical composition of coals, pertinent to high-temperature slagging, and how to use that information to infer slagging propensity information.

The working theory of the LIBS technique consists of the output from a pulsed laser focused onto a sample, optically induced plasma, called laser induced plasma (LIP), and a spectral detection system. The LIBS is formed when the laser power density

exceeds the breakdown threshold value of the sample surface. The spectrally and temporally resolved detection, and subsequent determination of the specific atomic emissions will reveal analytical information about the elemental composition of the sample. Since the 1980's, LIBS has been investigated for elemental determination in a variety of samples, including solid, liquid and gases. [1.1]

In LIBS, the sample atoms are excited to an excited state(s) and spontaneously emitted or radiated back to a lower state(s), usually the ground state. The intensity of return to the lower state is directly proportional to the concentration or number of atoms in the ground state. The probability of the transitions from a given energy level is expressed in the form of three coefficients, termed transition probability: A_{ji}, spontaneous emission, B_{ij}, spontaneous absorption, and B_{ji}, stimulated emission, which can be considered as representing the ratio of the number of atoms undergoing a transition to an upper left to the number of atoms in the initial or lower level and can be represented as follows:

$$N_j = N_0 g_i / g_0 \exp(-\Delta E / KT) \qquad (1.1)$$

Where the N_0 is the number of atoms in the lower state (ground state in most analytical situations), N_j is the number of atoms in the excited or upper level, g_i and g_0 are the statistical weights of the j^{th} upper state, and 0, the ground state, respectively. ΔE is the difference in energy in Joules between these two states, K is the Boltzmann constant ($1.38066 \times 10^{-23} J/K$) and T is the absolute temperature.

If self-absorption is neglected, then the intensity of the spectral emission, I_{em}, is

$$I_{em} = A_{ji} h\nu_{ij} N_j \tag{1.2}$$

Where h is the Planck's constant ($6.624 \times 10^{-34} Js$), ν is the frequency of the transition). Therefore, N is directly retted to the concentration in the sample as follows:

$$N_j = N\, g_i / g_0 \exp(-\Delta E / KT) \tag{1.3}$$

The emission intensity of a spontaneous emission line or wavelength, I_{em}, is related to this equation (sometimes called the Maxwell-Boltzmann Equation) as follows:

$$I_{em} = A_{ji} h\nu_{ji} N\, g_i / g_0 \exp(-\Delta E / KT) \tag{1.4}$$

The atomic emission intensity is dependent on temperature and wavelength. Thus, a higher temperature at a longer wavelength would give the most intense atomic emission signal.

The experimental set-up for the LIBS techniques is relativity compact compared to other analytical instrumentation such as mass spectrometry, laser-induced fluorescence (LIF), inductively coupled plasma-atomic emission spectrometry (ICP-AES), etc. The LIBS system is comprised of a chamber for sample introduction, as well as plasma generation; a laser source; and a detection system for plasma emission. More details will be covered in the Experimental Setup Chapter. A schematic diagram of a conventional LIBS experimental system is shown in Figure 1.1.

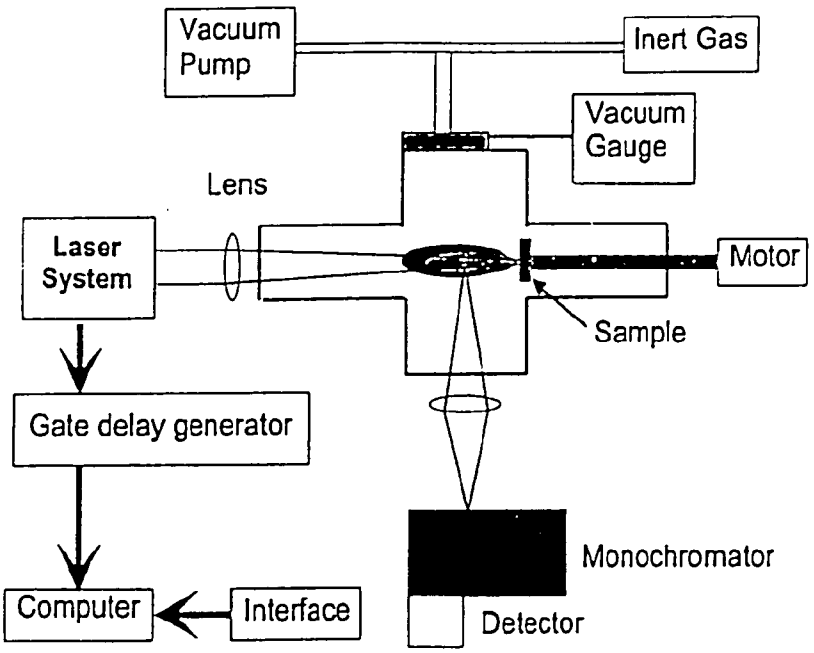

Figure 1.1: Schematic Diagram of a Conventional LIBS Experimental Setup

In most of the analytical LIBS experiments performed in the laboratory, the chamber is an essential part in the plasma generation. This is due to the fact that most analytical experiments for LIBS are performed with a buffer gas. The chamber is generally made of aluminum or stainless steel. The chamber should have at least three windows, one for laser introduction, one for detection of the spectral emission and one for monitoring the generation of the plasma. The emission signals are typically delivered to the entrance slits of different monochromators, which are used to differentiate the light signals by their wavelengths.

The characteristics of the laser-induced plasma, such as intensity, length,

lifetime, etc. vary by changing the pressure of the experimental chamber. Therefore, precise monitoring of the buffer gas pressure is a crucial part of the experiment. According to the referenced experimental results on the efficient generation of the laser-induced plasma, an argon or helium atmosphere is better suited in producing a more intense plasma generation compared to an air atmosphere, and vacuum conditions are better suited than an air atmosphere.

In analyzing LIBS signals, measurement accuracy is frequently defined as how close the measured experimental value is to the 'true' or accepted value. It is most frequently obtained by comparison to a standard or group of standards. These standard values have been obtained by independent analytical techniques. These standard reference materials (SRMs) allow a characterization of error. In practice the SRMs rarely exactly match the components of an unknown sample. The choice of SRM should meet three criteria: it should have a comparable or similar matrix, the sample concentrations should be about the same, and the uncertainty in the SRM certified concentration should be lower than the specified left of bias for the determination. [1.1] The precision of LIBS measurements depends on the complexity of the sample, homogeneity of the sample, and the reproducibility of the laser shots. Typical values are in the 1 to 10 percent range.

Chapter 2: Literature Review

2.1 Slagging Indices

Coal contains mineral matters which can, in combustion systems at suitably high temperatures, form slagging, and can cause fouling too. Coal plants which are designed to burn pulverized coal are able largely to accommodate these problems. Slagging is defined as deposition of fly ash on heat-transfer surface and refractory in the furnace volume and upstream tube banks primarily, subjected to radiant heat transfer. Although the name 'slagging' suggests a fused or semi-fused ash, the term slagging may also apply to sintered deposits and dry ash formed in oddly sized, low-pressure steam generator furnaces, or in furnaces fired with coals containing high moisture and alkaline earth ash. Fouling is defined as deposition in the heat-recovery section of the steam generator subject to convective heat exchange by fly ash quenched to a temperature below its predicted melting point, condensation by volatiles, or sulfidation by sulphur oxides. These deposits may vary from light sintering to complete fusion; the latter is due to the formation of lower melting sulfates.

Fouling and slagging are very complex phenomena. A good body of literature has been reported in the field of slagging and fouling that focused on slagging indices in a variety of coals and combustion systems. Slagging indices are of interest, since they can help coal-fired power plant operators to rate different fuels according to their propensity to deposit in the different regions in the boiler. Some slagging indices apply to a broad range of coals and combustion systems, while others have very limited applicability. It

is important to recognize that the extent and relative importance of a given index varies from boiler to boiler, and mine to mine. Take an important index, base/acid ratio for example, for some boilers and coal a base/acid value of 1.1 may be an indication of light slagging deposition. However, for some other boilers, this value would cause serious depositions on the furnace and screen cubes. Thus, it is important to decide on a proper index, which has a good coverage of coal properties and applicability for a good range of coals. Furthermore, the recommendations for a particular index, in terms of its ranges for high, medium and low slagging potential should be adjusted on a per-boiler basis.

A major problem in developing ways to predict ash behavior is the high variability and complex associations of the inorganic components in coal. The association and abundance of major, minor, and trace elements in coal is dependent upon the coal rank and depositional environment. Inorganic components in lower-rank sub-bituminous and lignite coals are associated with the organic and mineral portions of the coal matrix. Lower-rank coals contain high levels of oxygen, some of which are in the form of carboxylic acid groups that can act as sites for alkali and alkaline earth elements. Unlike lower-ranked coals, the inorganic components associated with bituminous and anthracite coals are primarily in the form of minerals. These major mineral groups include quartz, clay minerals, pyrite, and carbonate minerals. [2.1]

The most widely used high temperature slagging prediction descriptor, is the base-to-acid ratio, base and acid are simply the sums of the weight percentages by mass of the basic and acidic oxides in the ash. [2.2]

$$\text{Base} = Fe_2O_3 + CaO + MgO + K_2O + Na_2O \quad (2.1)$$

$$\text{Acid} = SiO_2 + Al_2O_3 + TiO_2 \quad (2.2)$$

$$B/A = \text{Base} / \text{Acid} \quad (2.3)$$

For coals with a bituminous type of ash (pyrochemically acidic ashes, where $Fe_2O_3 > CaO + MgO$ and/or $SiO_2 > Fe_2O_3 + CaO + Na_2O$), the base/acid ratio is often used as an indicator of the tendency of ash to form low melting point eutectics, which is then stickier at a lower temperature. It is suggested that the low melting point eutectic tends to form at a base/acid ratio of 0.5 and, since the base/acid ratio for most bituminous type ashes is below this value, a base/acid ratio higher than 0.5 is an indication of increased slagging deposition potential. Increasing the base/acid ratio generally results in decreased deposit viscosity until a minimum viscosity is reached at a base/acid ratio of 1.0. The base/acid ratio was empirically formulated; however, it has a sound base, since the oxides considered as acids and bases correspond to the elements generally acting as viscosity-increasing network formers and viscosity-decreasing network modifiers. As the most widely used index, the base/acid ratio has been applied to a large ranges of combustion analysis, to predict slagging propensity. Coals with severe slagging propensity fall in the range of base/acid ratios greater than 1.75; coals with a base/acid ratio between 1.0 and 1.75 has high slagging propensity; coal with base/acid ratio between 0.5 and 1.0 has medium slagging; while coals with a very light slagging propensity ranked at base/acid ratios smaller than 0.5.

Several other empirical indicators have been proposed. A standard index for a coal of a bituminous type ash is the product of the sulfur content and the base/acid ratio.

The sulfur content is an indication of the quantity of pyritic iron in the mineral matter and this influences the degree of oxidation of iron in the slag, affecting its slagging behavior. This index attempts to estimate the tendency for particles to adhere because of their inherent stickiness. Attig and Duzy [2.3] are attributed an empirical slagging index by multiplying the base to acid ratio by dry sulfur in the coal:

$$\text{Slagging Index, Fs} = \text{dry S\%} * \text{B/A} \qquad (2.4)$$

Coals with a low slagging potential should have for this index Fs values of less than 0.6. If the Fs value falls between 0.6-2.0, it stands for medium slagging; while 2.0-2.6 represents a high slagging potential. When Fs value is greater than 2.6, slagging is severe.

Other ash chemical components different than those included in the base/acid ratio play an important role in the slagging and fouling phenomena. The ash chemistry of most coals shows high levels of silica and aluminum. When reported as oxides, most of the time these two elements make up for up to eighty to ninety percent of the ash. Another noteworthy index, is the Silica percentage. As described by Winegartner [2.4], a silica percentage is used as an index and expressed as:

$$\text{Silica \%} = \frac{SiO_2}{SiO_2 + Fe_2O_3^{*} + CaO + MgO} * 100\% \qquad (2.5)$$

$$\text{Where} \quad Fe_2O_3^{*} = Fe_2O_3 + 1.11\ FeO + 1.43\ Fe^{0} \qquad (2.6)$$

The values of the oxides are in weight percent (by mass). The use of the silica ratio requires knowing the amount of iron in each oxidation state, which is normally obtained by an analysis of the ash. However, for the purposes of these calculations, the

equivalent Fe_2O_3 is taken to be the value of Fe_2O_3 in the ash, with no Fe^{+2} and Fe^0 present (because of full combustion). The slagging potential in terms of the silica ratio is: for silica ratios above 72 percent, light slagging; for silica ratio from 65 percent to 72 percent, medium to high slagging takes place; and when the silica ratio is less than 65 percent, slagging is severe.

In most cases, ferric oxide is the third most abundant element, and the highest percentage of the metal oxides. It is commonly assumed that the iron oxide level of all the coals that cause limited slagging is below 8 percent. Those coals deemed to have iron oxide levels greater that 15 percent cause severe slagging. A coal that has an intermediate slagging performance has an iron oxide level between 8 and 15 percent.

An I/C index is defined as:

$$\frac{I}{C} = \frac{Fe_2O_3}{CaO} \tag{2.7}$$

Values of the I/C ratio between 0.3 and 3.0 correspond to low-viscosity eutectic mixtures, which contribute to heavy slagging. With the I/C value greater than 3.0 or less than 0.3, the slagging is slight. [2.5]

Another important index for slagging is the ash fusion temperature (AFT). AFT of coals and coal blends is one of the parameters currently widely used in coal marketing and assessment of coal quality, coal ash fusibility and melting characteristics. The AFT contains four temperatures representing four stages of the coal deformation. The initial

deformation temperature stands for the temperature when coal begins to deform; the softening temperature is when deformation happens on the whole coal particle; the hemispherical temperature stands for when the coal particles turn the shape of a hemisphere on their edges; and fluid temperature stands for when the coal particles exist in the fluid phase. To best represent the AFT as a slagging index, a combination of ash fusion temperatures is used into Ti, which is defined as follows:

Ti = 0.8*Initial deformation temperature+0.2* Hemispherical temperature (2.8)

When Ti is greater than 2,449 deg F, the slagging phenomena is slight; when Ti is between 2,250 and 2,449 deg. F, there is a medium slagging; when Ti is between 2,100 and 2,250 deg. F, slagging is heavy; below 2,100 deg. F, slagging is severe. [2.6]

Another reference, Maria Mastalerz et al., [2.7], has used several fouling indices involving Na_2O as in Table 2.1:

Table 2.1: Several Fouling Indices and Range of Values

Fouling Indices	Range Of Values		
	Low	Medium	High
(Base/Acid) * $Na_2 0$	<0.2	0.2~0.5	>0.5
($Na_2 0$ + 0.659 $K_2 0$)	<0.3	0.3~0.5	>0.5
% $Na_2 0$	<0.5	0.5~1	>1
% Cl	<0.3	0.3~0.5	>0.5
%SiO_2/%Al_2O_3	<2	>2	

One last reference, Skorupska [2.2] has summarized an index for slagging based on the silica to alumina ratio, as follows:

$\%SiO_2/\%Al_2O_3$ <2 low

>2 medium and high

Table 2.2: A Summary of All Slagging and Fouling Indices Listed in Chapter 2

		Low	Med	High	Sever
Base/Acid Ratio	Base=Fe_2O_3+CaO+K_2O+Na_2O+MgO Acid=SiO_2+Al_2O_3+TiO_2	<0.5	0.5-1.0	1.0-1.75	>1.75
Rs	Slagging Index, Rs = dry S% * B/A	<0.6	0.6-2.0	2.0-2.6	>2.6
Silica Ratio	Silica % = $\frac{SiO_2}{SiO_2 + Fe_2O_3^* + CaO + MgO} * 100\%$ Where $Fe_2O_3^* = Fe_2O_3 + 1.11\ FeO + 1.43\ Fe^0$	72-80	65-72	65-72	50-65
Iron/ Calcium Ratio	$\frac{I}{C} = \frac{Fe_2O_3}{CaO}$	<0.31 OR >3.0		0.31-3.0	
	(Base/Acid) * $Na_2 0$	<0.2	02-0.5	>0.5	
Alkaline Metal Content In Ash	($Na_2 0 + 0.659\ K_2 0$)	<0.3	03.-0.5	>0.5	>0.5
Sodium in Ash	% $Na_2 0$	<0.5	0.5-1.0	1.0-2.5	>2.5
Chlorine in Coal	% Cl	<0.3	0.30-0.5	0.3-0.5	>0.5

2.2 LIBS Applications

For the purpose of investigating the feasibility of using LIBS for coal chemical analysis and infer the slagging tendency of coals, it would be very useful to search previous studies performed in this related area. The application of LIBS is still incipient; however, some practical work had been performed in coal samples.

In a study by Ottesen, DK et al., [2.8], laser spark emission spectroscopy was used to characterize individual coal particles in flowing environments. Nearly all of the inorganic constituents present in coal above a concentration of 100 ppm were observed in the laser spark emission from single particles. Several aspects of the technique are mentioned by Ottensen, et al., (1) the plasma excitation process; (2) experimental intensities and methods of calculating elemental composition; and (3) the comparison of particle-by-particle results with average bulk chemical analyses and scanning electron microscopy data. This work reports the first direct experimental comparison of composition on a particle-by-particle basis with grain-by-grain determination of elemental ash composition.

In a study of fly ash unburned carbon analysis, by Miki Kurihara et al., [2.9], the LIBS technique was applied to the detection of unburned carbon in fly ashes. An automated LIBS unit was developed and applied to a 1000 MW pulverized coal-fired power plant for real-time measurement of unburned carbon in the fly ash. Good agreement was found between measurement results from the LIBS method and those

made with the conventional method (Japanese Industrial Standard 8815), with a standard deviation of 0.27 percent. This result confirms that the measurement of unburned carbon in fly ash by LIBS could be accurate enough for using in coal-fired power plants. Measurements taken by this apparatus were also integrated into a boiler-control system with the objective of achieving optimal and stable combustion.

Fiona J. Wallis, et al., [2.10] used LIBS for the chemical analysis of low-ash lignite coals. An Nd: YAG (neodymium-doped yttrium aluminum garnet) laser (with a wavelength of 1064 nm) was used to induce emission from the ash-forming components, which was then spectrally resolved and analyzed. LIBS analyses of five inorganic components in lignite coal were shown to be reproducible between sample pellets at a 95 percent confidence level. Detection limits (in ppm) on an as-received basis of 60 (Ca and Al), 70 (Na), 90 (Fe), and 200 (Mg and Si) were obtained from the study of 30 lignite samples, each of which was interrogated by 300 laser pulses.

In another research using the LIBS technology by Doug Body and Bruce L. Chadwick [2.11], LIBS was allowed for the simultaneous determination of all detectable elements using a multiple spectrograph and synchronous, multiple charge coupled device spectral acquisition system. The device was designed to reduce the cost penalties associated with the application of LIBS while allowing accurate and precise determination of the elemental composition in coal. The system was particularly suited for the analysis of heterogeneous materials such as coal and mineral ores. For the coal analysis detectable elements included the key inorganic components of coal—such as Al,

Si, Mg, Ca, Fe, Na, and K—in addition to C and H. Detection limits varied depending on the particular element, but were typically of the order of 0.01 percent for as received, moist samples. Measurement repeatability and accuracy were typically within 10 percent absolute, which is similar to results from standard analysis procedures for heterogeneous materials.

In a research of industrial boilers at high temperatures, Linda G. Blevins et al., [2.12], applied LIBS near the superheater of an electric power generation boiler burning biomass, coal, or both; and at the exit of a glass-melting furnace burning natural gas and oxygen; and near the nose arches of two paper mill recovery boilers burning black liquor. Difficulties associated with the high temperatures and high particle loadings in these environments were surmounted by the use of novel LIBS probes. Echelles and linear spectrometers coupled to intensified CCD cameras were used individually and sometimes simultaneously. Elements including Na, K, Ca, Mg, C, B, Si, Mn, Al, Fe, Rb, Cl, and Ti were successfully detected in the experimental environment.

Another LIBS-based approach in coal analysis was taken by a group of Chinese researchers. Yu Liangying et al., [2.13], presented their results and discussions in "Analysis of Pulverized Coal by Laser-Induced Breakdown Spectroscopy". Their LIBS experimental results show a slope calibration curve nearly 1 when the concentration of analyzed elements is relatively low, and a slope of curve of nearly 0.5 when the concentration of C was higher than other elements. They concluded that the decrease of powder particle size lead to a remarkable increase of the plasma temperature.

Using the same technology as Yu Liangying, M. Noda et al., [2.14] from Japan also performed detection experiments of carbon content in coals by LIBS. In their experiments, Noda et al., applied LIBS to detect the carbon content in pulverized coal and fly ash under high-pressure and high-temperature conditions that characterize gasification thermal power plants. The results obtained using LIBS were compared to those from conventional methods for calorific value and the applicability of LIBS in the context of actual plant conditions were discussed. In their research, they concluded that LIBS featured a detection time capability of less than 1 min, compared to the sampling and analysis time of over 30 min required by the conventional method. This reference concluded that LIBS offers various merits as a tool for actual power plant monitoring.

In 1995, Zhang, Hansheng [2.15] and other researchers in the same research group from Mississippi State University, applied LIBS in a particle-loaded methane/air flame setup in the Diagnostic Instrumentation and Analysis Laboratory at Mississippi State University, to evaluate the application of LIBS on practical environments. The LIBS spectra collected from different observational directions and spectral regions were compared. The forward LIBS technique was chosen to characterize the upstream region of a large magneto hydrodynamics (MHD) coal-fired flow facility (CFFF). The relative concentrations of several species were inferred by fitting the observed CFFF LIBS spectra with computer-simulated spectra. Their paper reported the first LIBS experiments in a harsh, turbulent, and highly luminous coal-fired MHD environment. Their work demonstrated the LIBS capability in a MHD combustion environment.

Chapter 3: Experimental Setup

3.1 Experimental Setting Introduction

This chapter reports on the LIBS experimental setup used at the Energy Research Company (ERCo), Staten Island, NY, to test the feasibility of the LIBS technology to measure the coal chemistry of interest for high-temperature slagging determination. The idea is that with further research, this technology could be integrated at a coal-fired power plant, at the coal feed stream, in a concept shown schematically in Figure 3.1. In Figure 3.1, a laser beam is directed onto the surface of the coal stream, as it is fed into the mills. The laser vaporizes and ionizes micrograms of the feedstock. After a few microseconds the plasma cools whereupon the emitted radiation is collected by a spectrometer. The spectrometer records the wavelength and the intensity of the radiation. The wavelengths uniquely identify each element and the intensities determine their concentrations. With this method, it will be possible to monitor in real-time coal composition.

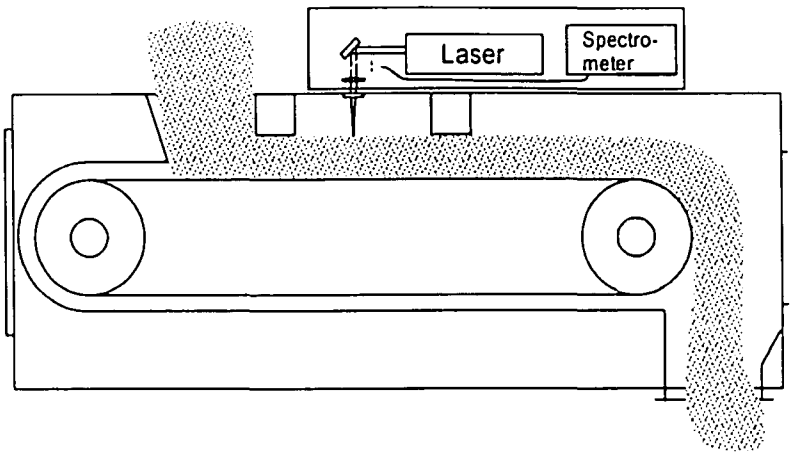

Figure 3.1: Schematic of the LIBS System

1. The experiment setup for the LIBS measurements was designed to accomplish:
2. Sparking of the sample with a laser under a controlled atmosphere to generate plasma sparks.
3. Movement of the sample for the fresh sample to be sparked with progressive laser shots.
4. The collection of the spectra from the spark with either an Echelle or Acton spectrometer and a photodiode array.
5. The collection of light intensity time traces for wavelength ranges corresponding to specific elemental emission lines.

To achieve these experimental objectives, a setup was designed and assembled from off-the-shelf and custom made components. The general layout showing the

connections between these components is provided in Figure 3.2. Working together, these components create a laser spark from a sample; collect spectra in a specific time window, as well as the required photodiode traces. The setup controls the time window allowed for specific emission lines to be observed from the plasma. This timing window is defined by a delay (time to start data collection after the laser spark) and a gate width (duration of data collection).

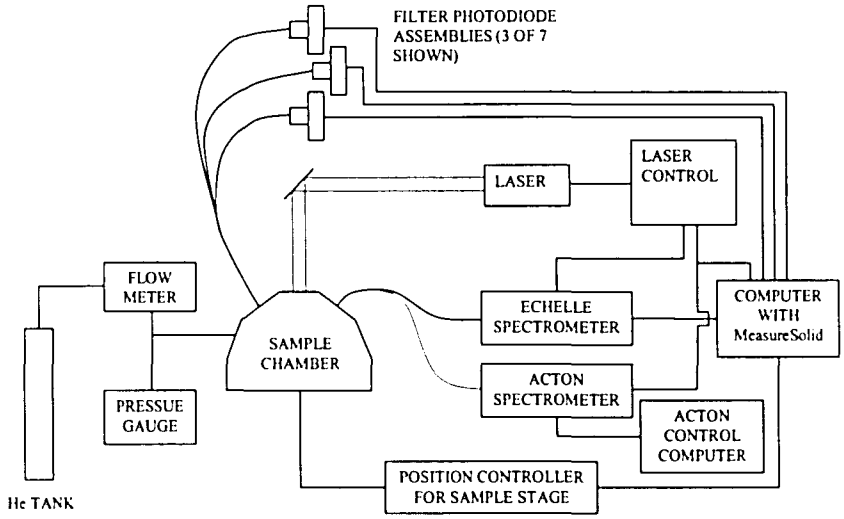

Figure 3.2: General Layout of System Components

The following is a description of the various components used in the experimental setup:

3.2 Experimental Instruments

3.2.1 Laser and Laser Control

Nd:YAG (Nd:Y3Al5O12) is a crystal that is used as a lasing medium for solid-state lasers. The Nd:YAG laser is very commonly used in optics researches. A Q-Switch Nd:YAG laser with pulse energies of approximately 100 MJ at 1064 nm and 180 MJ at 532 nm was used to generate the laser sparks on the sample. The triggering of a flash lamp and the Q-switch were externally controlled by an Echelle spectrometer. The time from the flash lamp trigger to the Q-switch trigger sets the power of the laser. At the time of the Q-switch trigger, the laser fires and creates the plasma spark on the sample. The laser is directed into the sample chamber using an adjustable mirror to accurately position the laser through the focusing lens.

The laser, a Big Sky Laser (Bozeman, MT) model CFR-400, emits coincident UV, visible, and near infrared laser pulses. The UV pulses were not used and were directed down into the beam dump by a 266 nm beam splitter. The visible and near infrared pulses were directed down into the chamber by the 1064 nm and the 532 nm laser mirror. A f/4 lens focuses the pulses onto the surface of the coal sample to create the LIBS spark. A picture of the laser system is shown in Figure 3.3. Figure 3.4 shows the laser controller and the laser generator.

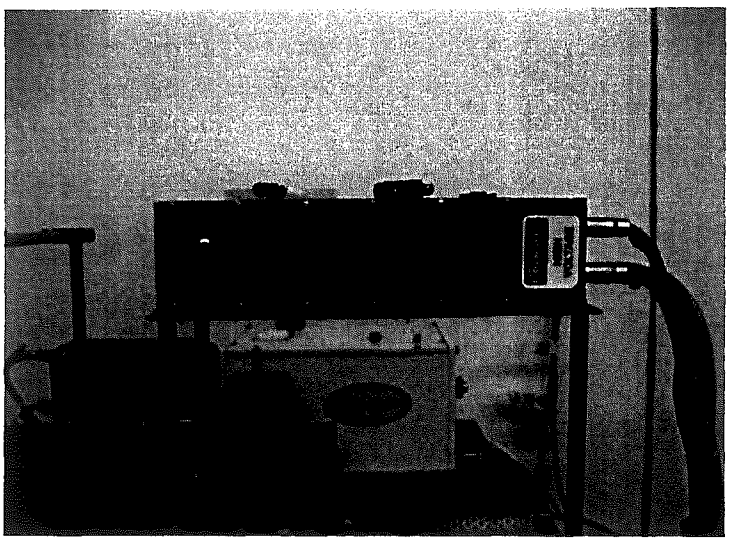

Figure 3.3: Big Sky Laser (Bozeman, MT) Model CFR-400

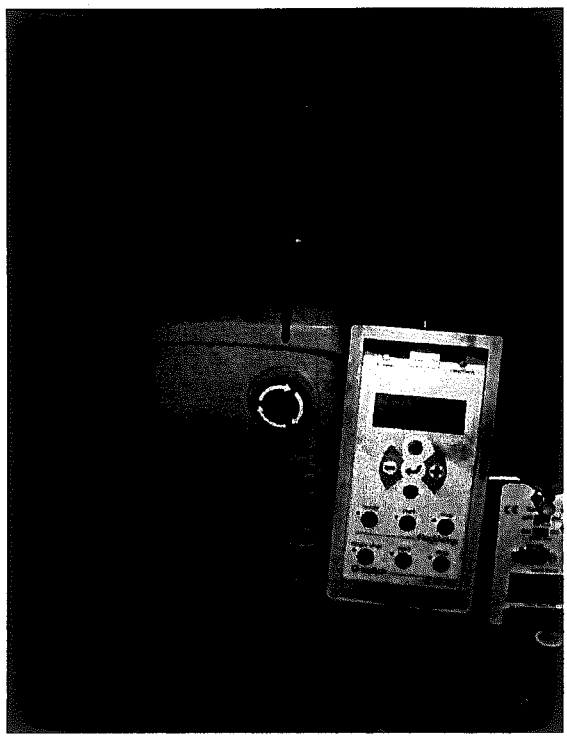

Figure 3.4: Laser Sparks Generator and Laser Controller

3.2.2 Sample Chamber

The sample chamber is the central part of the whole experimental system. This sample chamber controls the atmosphere surrounding the sample during the measurements and provides the movable stage, for the sample to move between lasers sparks. The laser is shot on the coal sample held by a container held in the chamber, in a non-oxygen environment to prevent errors caused by the elements in the air, and also to significantly reduce the coal sample combustion (combustion of the coal could still

slightly happen with the oxygen contained in the coal itself). This requires the chamber to be filled with an inert gas. Thus, the sample chamber controlled the atmosphere surrounding the sample during the measurements and provided the movable stage. A detailed diagram of the sample chamber is shown in Figure 3.5, while a photograph with labels is included in Figure 3.6.

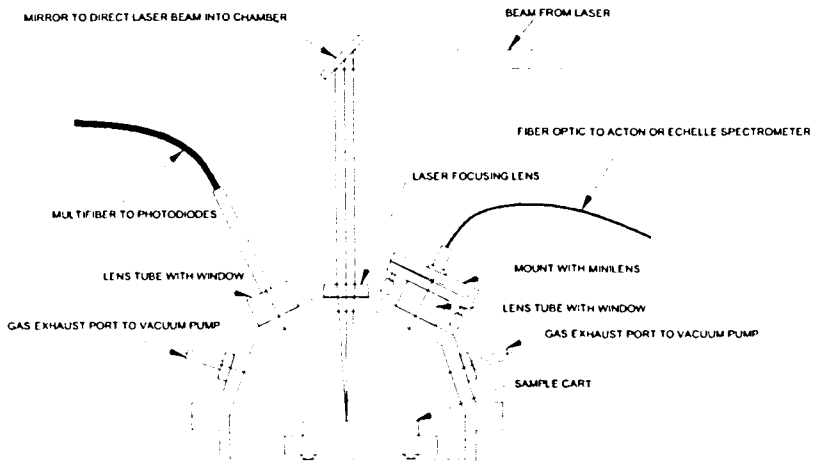

Figure 3.5: Diagram of Chamber for Coal LIBS Experiments

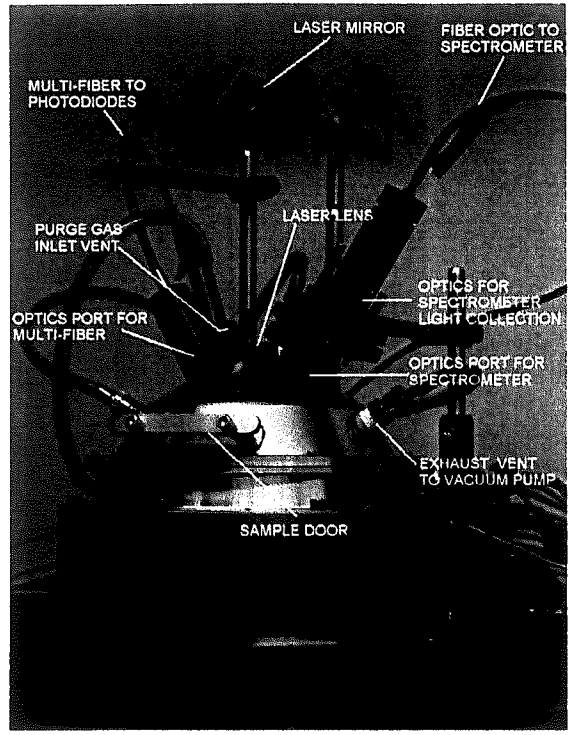

Figure 3.6: Overview of Sample Chamber

The main body of the chamber is composed of two pieces machined from aluminum. These pieces are held together with screws. An O-ring between the pieces insures a gas tight seal. The top portion of the chamber contains ports to control the atmosphere, introduces the laser into the chamber, and allows the viewing of the plasma by the optical instrumentation.

The vents into the chamber consist of o-ring fittings that form gas tight seals around ¼" stainless steel tubes. The inlet vents are near the optics port at the top of the

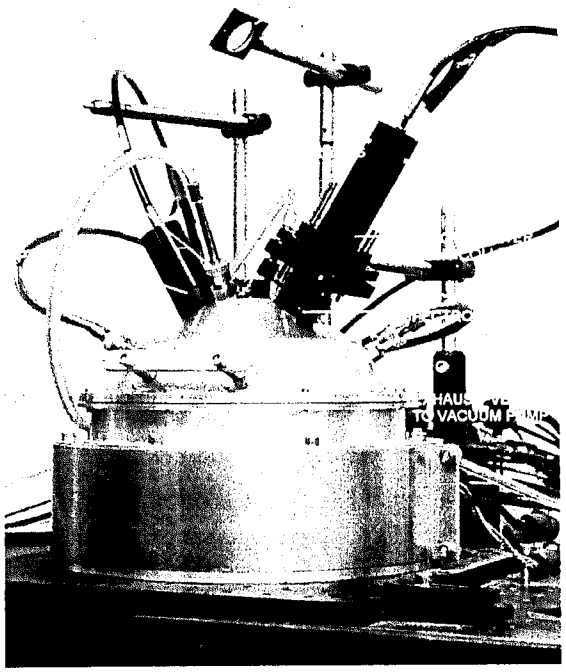

Figure 3.6: Overview of Sample Chamber

The main body of the chamber is composed of two pieces machined from aluminum. These pieces are held together with screws. An O-ring between the pieces insures a gas tight seal. The top portion of the chamber contains ports to control the atmosphere, introduces the laser into the chamber, and allows the viewing of the plasma by the optical instrumentation.

The vents into the chamber consist of o-ring fittings that form gas tight seals around ¼" stainless steel tubes. The inlet vents are near the optics port at the top of the

chamber and are directed to sweep the particulate from the laser spark away from the laser window. The exhaust ports are connected to a vacuum pump to remove gas and particulate from the chamber. During the measurements, the chamber is first pumped down to remove the air. While the pump continues to evacuate the chamber, a valve is then opened to allow helium gas to flow into chamber. The helium pressure, monitored with a pressure gauge, is set by a needle valve on the flow meter. During the measurements, the helium flow through the chamber remains to purge the system.

Windows with O-ring seals were placed in all of the optics ports to insure that the chamber remains gas tight. To focus the laser onto the sample and create the plasma spark, a lens was mounted on the outside of the chamber in vertically adjustable mount. This allowed the lens focal point to be adjusted with respect to the sample surface. The light collection system for the multi-fiber to the photodiodes consists of simply directing the end of the fiber at the plasma spark with no additional optics. A mini-lens was used to focus the light onto the end of an optical fiber to direct the light into the spectrometers.

A sample door in the chamber allows the sample to easily be placed on the sample cart as shown in Figure 3.7 and Figure 3.8. Figure 3.7 and Figure 3.8 show the inside of the chamber with the sample cart. The sample cart was coupled to a motorized XY stage below the chamber with a magnet. During the measurement, a sample movement provides fresh sample for each laser shot. The position of the stage is set by the position controller for the sample stage with the positions preset by a software, called MeasureSolid.

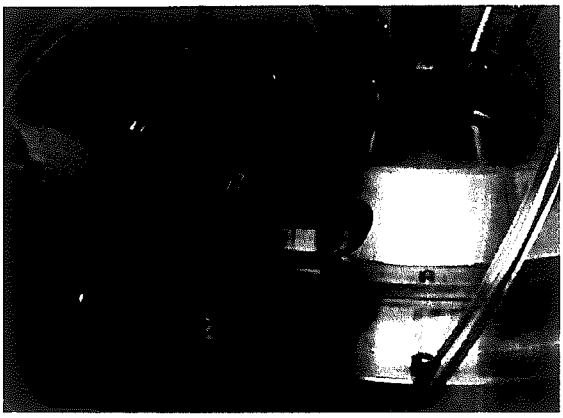

Figure 3.7: Loading of Sample Into Chamber.

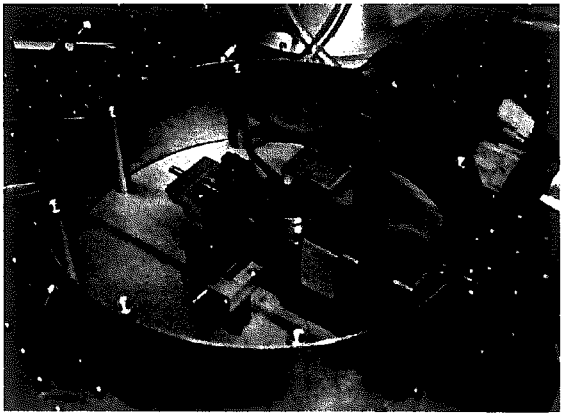

Figure 3.8: Inside of Chamber Showing Holder and Cart

3.2.3 Computer with MeasureSolid

The primary control of the measurement system is a computer with the

MeasureSolid Software. The MeasureSolid software was developed by ERCo to coordinate the activities of the various LIBS system components. During measurements on the coal samples, the MeasureSolid software sets the laser firing and spectrometer data collection parameters, controls the sample position and stores the spectrometers trace data. This computer was also equipped with an A/D board to collect data from the photodiode assemblies. A picture of the controlling computer is shown in Figure 3.9.

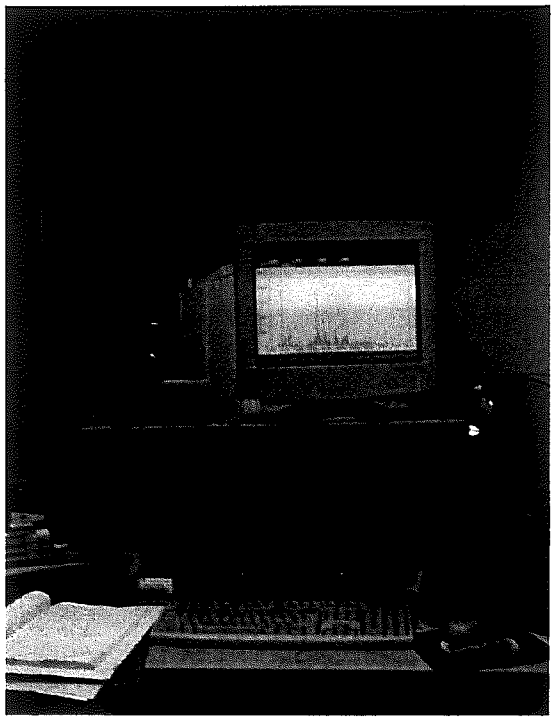

Figure 3.9: Controlling Computer

3.2.4 Echelle Spectrometer

The primary role of the Echelle spectrometer (ESA 3000 LLA, Germany) is to collect spectra data for the analysis of metals in the coal samples. This spectrometer contains an Echelle type grating that allows for high resolution spectra to be collected over a broad wavelength range (200 – 600 nm). The timing window for Echelle spectra collection is set by the MeasureSolid Software. Further, the Echelle spectrometer controls the firing of the laser.

3.2.5 Acton Spectrometer

An Acton spectrometer (SpectraPro 300i, 0.3 m grating spectrometer, Roper Scientific, NJ) equipped with a PI-Max Intensified CCD camera (PiMax, Princeton Instruments, NJ) was used to achieve the timing window required to observe the sulfur, S-II, emission lines from the plasma. The timing parameters for the spectra collection window and the number of spectra accumulated into a single spectrum from a sample are set from the Acton control computer, while the trigger for the data collection is received from the laser control unit. Due to the limited number of viewing ports on the sample chamber, only one spectrometer could be used to collected spectra at a time.

3.2.6 Filter/Diode Assemblies

The filter/diode assemblies were used to collect intensity traces as a function of time for the emission lines of C, H, O, N, S, and K. Interference filters (Andover

Corporation, NH) limit the wavelength range of the light reaching the photodiodes to that of the emission lines of interest. An additional filter diode assembly measures the background intensity of the plasma as a function time. The background wavelength range was selected to be void of emission lines from the coal. A summary of the emission lines and the filter center wavelengths and bandwidths are given in Table 3.1.

Table 3.1: Summary of Interference Filter for Emission Lines and Background

Species	Emission Line Wavelength (nm)	Filter Center Wavelength (nm)	Filter Bandwidth (nm)
C	940.6	941.0	2.08
H	656.3	656.8	2.76
O	777.4	777.8	2.96
S	921.3	921.7	2.84
N	868.3	868.3	0.56
K	769.9	769.9	2.14
Background		821.0	1.10

A Photodiode/amplifier unit (PDA55-Switchable Gain Amplified Silicon Detector, ThorLabs, NJ) measures the intensity of the filtered light. These units convert the light intensity passing through the filter to a voltage signal. Figure 3.10 shows a picture of the filter/photodiodes assembly. An A/D board on the primary computer records the voltage signal from the photodiodes as a function of time. A trigger from the laser control unit initiates the collection of the data at the time of the laser spark. The traces from the individual laser shots are stored in separate files on this computer.

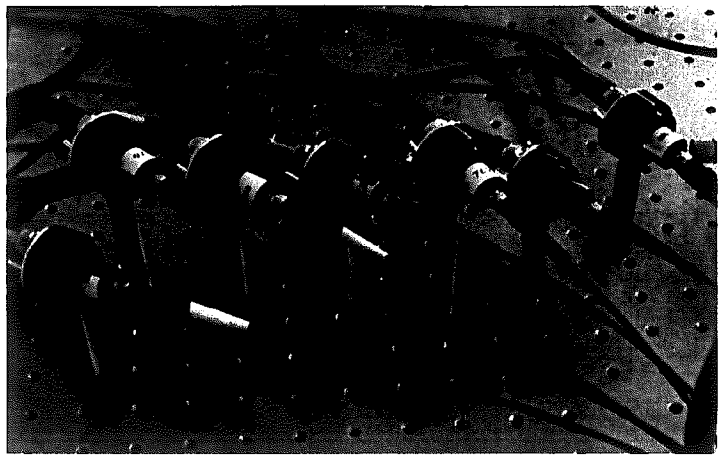

Figure 3.10: Photodiode Assemblies for Collecting Intensity Traces.

3.3 Sample Preparation

The samples for the LIBS measurements should be in the form of fine powders. The powders were mounted on double sided sticky tapes by placing a few tenths of a gram of powder on the tape and then distributing the powder over the tape with a plastic card. The powder on the tape was then gently scraped to remove any loose powder. This method was selected over other methods such as pressing the powders into pellets due time and work advantages, and the field tests response to this method was very satisfying. To reduce the error caused by unevenly distribution within the coal sample, samples were sorted using a rifler, dividing the sampling until a representative sample of 5 g was obtained for mounting on the tapes.

3.4 Measurements

In the LIBS experiments, every time the laser sparks on the coal sample in the chamber, it is considered a shot. After each shot, the emitted light signal is collected and recorded in the LIBS system. The signal strength can be controlled by the window open time. Different window open time lengths will generate different intensities at the same wavelength, and the results can be compared under different window open times to seek for the best setting for the best LIBS data. The best used for the window open time was 1 ms after spark happens and the shuts off 3.5 ms after the spark happens for data collecting. In the experiments, the laser gave 100 shots on different locations of one sample. These shots locations were basically a 10 by 10 matrix which covered most of the surface area of the sample. The data collecting software could automatically eliminate the bad shots, which could possibly be caused by the shots made on the tape or container itself or two shots on the same point. The collecting procedure took 12 to 15 minutes for each sample, and after eliminating the bad shots data from the 100 sets, an average file of all values was calculated. The whole procedure was executed to reduce as much error as possible caused by coal sample and equipment limitation. After 100 sets of data were collected, the laser sparking stops automatically, and then the pump and He filling should be stopped, returning the chamber pressure to normal, the chamber gate is opened and the sample is taken out.

Chapter 4: Modeling Results

4.1 Modeling for Fs

The purpose of this study is to develop predictive models for coal slagging propensity that could be used with data generated from a LIBS system. This chapter reports on the development of these models and their performance. Two specific indicators were used to predict slagging potential. The first indicator is the ash base/acid ratio times the sulfur content of the coal, or Fs. The Fs parameter was already described in Literature Review Chapter. The second indicator is the ash fusion temperature. Ash fusion temperature was also described in Literature Review Chapter and is one of the most common indicators utilized by boiler operators to anticipate the slagging behavior of the coals fired in their units.

In developing these predictive models to relate LIBS data to the slagging indices Fs and Ti, LIBS signals are used as model inputs, and the indices Fs and Ti are used as model outputs. The LIBS signals are the light spectral intensities at different wavelengths corresponding to different elements, these signals are recorded from the LIBS experiments. The Fs and Ti indices represent the coal slagging propensity. Therefore these models are actually an effective connection between the LIBS data and the high-temperature slagging phenomena. If these LIBS-based models are capable of correctly reproducing the slagging indices, they could be used in-situ and in real-time, with a LIBS system functioning at a power plant, to infer slagging behavior from a

variable coal feedstock.

To predict the Fs parameter, artificial neural networks (ANNs), were used in this study. In recent years, ANN has been proven very useful in the analysis of complex and uncertain data (which is a common feature of the LIBS data). A neural network is a system of interconnected processing elements, inspired by the network structure of the brain, which learns the relationship between input data vectors and the output(s). The networks are constructed by simple processing units or nodes connected together with parameters called weights. A weight indicates how strongly the source unit of the connection affects the value of the destination unit. The units in a neural network are usually arranged in layers, for example, an ANN generally consists of an input layer, an output layer, and several hidden layers of nodes (typically 1 to 2 hidden layers were used in the LIBS modeling data). Normally, the number of nodes in the hidden layers is determined by the user and in relation to the number of inputs and outputs. In this study to predict Fs, an advanced ANN model type, neurofuzzy model was used. This type of ANN model was used, given that the other more traditional ANN model algorithm tried, the feed-forward network, prove unsuccessful for this application.

Neurofuzzy is an ANN model type that can deal with explicit knowledge which can be explained and understood through a learning process. This learning process provides a way to adjust the given knowledge and automatically generates additional fuzzy rules and membership functions, to meet certain specifications and reduce the design time. On the other hand, the neurofuzzy logic enhances the generalization

capability of a neural network system by providing more reliable outputs when extrapolation is needed beyond the limits of the training data. Figure 4.1 shows a typical diagram illustrating a neurofuzzy network. The links between the network nodes in a neurofuzzy ANN has a fuzzy logic algorithm calculator. The ANN models for this study were built using the software "NeuFrame" [4.1].

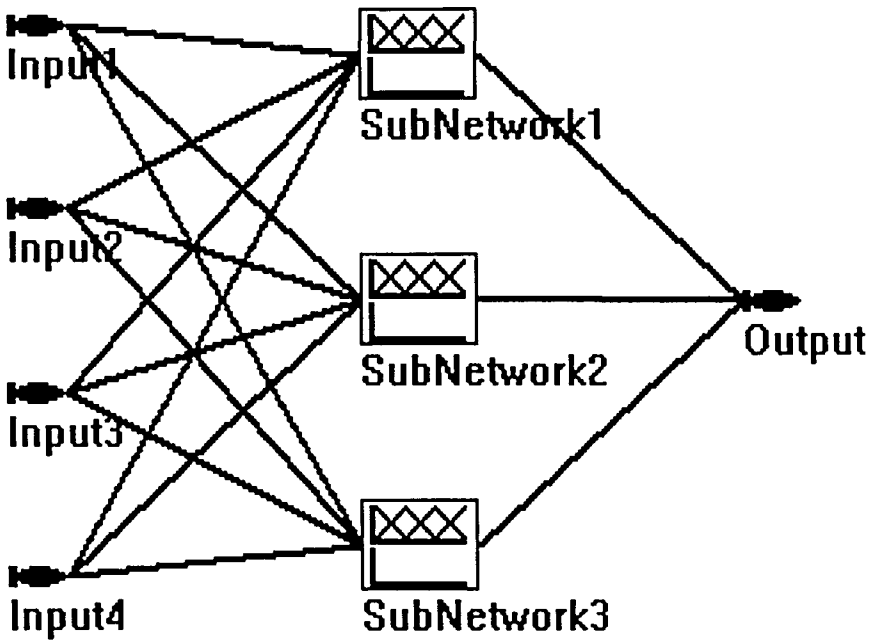

Figure 4.1: Diagram Illustrating a Neurofuzzy System

As indicated in the Literature Review Chapter, Fs is defined as the product of the ratio of the sum of all base species to the sum of all acidic species, times the sulfur content of the coal. This definition of Fs includes a combination of several major oxides concentrations, as well as the S concentration in the coal. Therefore nine elemental

spectral intensities from the LIBS signature were selected as the predicting ANN model inputs, including Mg, Ca, Na, K, Fe, Si, Ti, Al and S.

There are a few major features in the LIBS data that make ANNs suitable for building up slagging index predicting models. First, the intensity signal at a certain wavelength of a particular element is related to the real concentration of that element, but the connection between element LIBS intensity and weight concentration is very complex and non-perceivable; therefore, the intensity data cannot be used directly as a coal chemical property and needs to be processed before applied in a slaggind index. Thus, the neurofuzzy technique provides parallel processing characteristics, allowing it to develop complex functional relationships to deal with the LIBS data. Secondly, the LIBS intensities data for the nine elements, which are used as model building inputs, are highly non-linear, as well as dependent on a large number of the LIBS laser parameters. The neurofuzzy networks has learning characteristics, which make it ideal for adapting to different conditions of the LIBS data. Therefore, these inherent features of the neurofuzzy technique make it attractive for the LIBS data processing considered in this study.

4.2 Modeling for Ti

Another important slagging index, the ash fusion temperature Ti is commonly used by power plants and coal companies. To predict this slagging indicator, a mathematical method was introduced in this study too. A mathematical model worked

better than an artificial intelligence-based model. Because the chemical and mineralogical compositions of the coal ash can determine its melting characteristics and fusion temperatures, the idea was to relate ash fusion temperatures with LIBS-determined chemical composition. In this study, a mathematical model was developed using some key coal properties parameters. These input parameters, are: Si, Al, Ti, Fe, Ca, Mg, Na and K, the base/acid ratio the silica ratio, etc., these parameters were selected based on the important roles they play in the slagging phenomena. A combination of species concentrations and their cross products was believed to very well represent ash fusion temperature. It should be reiterated that to obtain a valid connection between the LIBS data and the slagging indicator Ti, all the oxides concentrations were replaced by their corresponding LIBS elemental intensities. The following combination of sixteen parameters was selected as the final input parameters for a fusion temperature model because of their predicting performance. Most the parameters are described in the form of oxides, but when building the actual model, corresponding LIBS intensities data were used:

1. Silica Value = $SiO_2 / (SiO_2 + Fe_2O_3 + CaO + MgO)$

2. Base = $Fe_2O_3 + CaO + MgO + K_2O + Na_2O$

3. Acid = $SiO_2 + Al_2O_3 + TiO_2$

4. $R_{250} = (SiO_2 + Al_2O_3) / (SiO_2 + Al_2O_3 + Fe_2O_3 + CaO)$

5. Dolomite Ratio = $(CaO + MgO) / (Fe_2O_3 + CaO + MgO + K_2O + Na_2O)$

6. Carbon weight percentage of the coal

7. Hydrogen weight percentage of the coal

8. Sulphur weight percentage of the coal

9. Heat value of the coal, BTU

10. Percentage of SiO_2 in coal ash

11. Percentage of $Al_2O_3+TiO_2$ in coal ash

12. Percentage of Fe_2O_3 in coal ash

13. Percentage of CaO in coal ash

14. Percentage of MgO in coal ash

15. Percentage of K_2O in coal ash

16. Percentage of Na_2O in coal ash

Both a linear and a non-linear regression analysis were used to develop correlations between LIBS-determined ash chemical compositions and the ash fusion temperature. The goal of the regression analysis was to determine a correlation for estimating the ash fusion temperature that best fit the set of data observations. The general appearance of the linear relation was assumed to be:

$$Y = \beta_1 + \beta_2 X_1 + \beta_3 X_2 + ... + \beta_{n+1} X_n \qquad (4.1)$$

Where Y is the dependent variable, β_1 to β_{n+1} are the equation parameters for the linear relation, and X_1 to X_n are the independent variables for this system. The general form of the linear relation obtained in this study is as follows:

$$T°(C) = l_1 + l_2[\text{Silica Value}] + l_3[\text{Base}] + l_4[\text{Acid}] + l_5[\text{Dolomite Ratio}] + l_6[\text{R250}] + l_7[\text{Carbon}] + l_8[\text{Hydrogen}] + l_9[\text{Surphur}] + l_{10}[\text{BTU}] + l_{11}[\text{Si02}] + l_{12}[\text{A1203}] + l_{12}[\text{Fe203}] + l_{14}[\text{CaO}] + l_{15}[\text{MgO}] + l_{16}[\text{K2O}] + l_{17}[\text{Na20}] \quad (4.2)$$

Since there is no direct solution for Equation 4.2, a MATLAB 7 program was written for determining the linear equation Coefficients, l_1 to l_{17}. A section of the MATLAB code is shown below, it is designed to calculate the coefficients for predicting a linear relationship model for Ti. After running the MATLAB code, the predicted Ti values are exported to a worksheet for future comparisons with actual Ti values. Red texts annotated below are explanations for each section of the code and they are not involved in the calculations.

```
A = data(:,17);              * "data" is the matrix file for sixteen input dependences.
B = [ones(3672,1),data(:,1:16)];   *the input group has 3672 coal samples
C = inv(B'*B)*B'*A           * soluting the coefficients vector, l1 to l17
D = [ones(448,1),data1(:,1:16)];    * "data1" is the matrix file for sixteen input
                             *dependences., the comparing group has 448 coal samples.
E = D*C;                     *E is the predicted vector to be compared with actual Ti values
```

A non-linear relation for Ti was also investigated in the form of:

$$Y = \alpha_1 (X_1)^{\alpha_2} (X_2)^{\alpha_3} \ldots (X_n)^{\alpha_{n+1}} \quad (4.3)$$

Where α_1 to α_{n+1} are the equation parameters for the non-linear relation. X_1

to X_n are the independent variables for this system. The general non-linear relation defined in this study, is:

$$T^{o}(C) = c_1[\text{Silica Value}]^{c_2}[\text{Base}]^{c_3}[\text{Acid}]^{c_4}[\text{Dolomite Ratio}]^{c_5}[\text{R250}]^{c_6} [\text{Carbon}]^{c_7}[\text{Hydrogen}]^{c_8}[\text{Surphur}]^{c_9}[\text{BTU}]^{c_{10}}[\text{Si02}]^{c_{11}}\ [\text{A1203}]^{c_{12}} [\text{Fe203}]^{c_{13}}[\text{CaO}]^{c_{14}}[\text{MgO}]^{c_{15}}[\text{K2O}]^{c_{16}}[\text{Na20}]^{c_{17}} \quad (4.4)$$

Similarly, MATLAB 7 was used for determining the non-linear equation Coefficients, c_1 to c_{17}. A section of the MATLAB code for the non-linear case is shown below. It was designed for calculating the coefficients for predicting the non-linear relationship model for Ti. After running the MATLAB code, predicted Ti values are exported to a worksheet for future comparisons with actual Ti values. Again, the red texts are explanations for each section of code, they don't involve in the calculations.

```
A=log(data(:,17));              * "data" is the matrix file for sixteen input
                                  dependences.
B=[ones(3672,1),log(data(:,1:16))];   *the input group has 3672 coal samples
C=inv(B'*B)*B'*A                * soluting the coefficients vector, C1 to C17
D=[ones(448,1),log(data1(:,1:16))];    * "data1" is the matrix file for sixteen
                *input dependences., the comparing group has 448 coal samples
E=D*C;
F=exp(E);   *F is the predicted vector to be compared with the real Ti values
```

Before applying the models described in the proceeding text to LIBS data, a test was performed using historical data. This procedure was done to check whether the Fs neurofuzzy and the Ti mathematical models would do a good job in predicting these slagging parameters using laboratory coal chemical analysis. This procedure was also used to tune the models. For this simulation step, the U.S. Geological coal database [4.2] was used. This database contains a complete record of coal property data, including 136 fields of coal properties and 7,432 coals samples mined in the U.S. In this database, chemical data for the samples are presented on an "as received, whole coal" basis. Due to the deficiency of the data source and lack of field testing techniques, some fields contain no data or contain negative zero values; however, the samples with such fields were manually erased from the database for use in this test. Table 4.1 shows an example of the data contained in this database. The data imported from this database are in the form of weight concentrations of the related elements. i.e., iron ppm_w ratio in the coal.

Table 4.1: Some Area of the U.S. Geological Coal Database

SAM.	STATE	BTU	AFT	MOISTR	V.MAT	FIX.C	S
211739	NEW MEXICO	7888	2800	12.80	28.20	30.70	0.50
211742	NEW MEXICO	9012	2800	12.30	33.00	34.00	0.50
240993	WYOMING	9957	2170	17.84	28.36	45.53	0.56
211743	NEW MEXICO	9990	2800	15.80	32.40	40.20	0.50
201446	COLORADO	10934	2910	9.50	31.40	49.50	0.90
174717	KENTUCKY	11480	1990	3.90	41.20	39.30	0.80
218688	VIRGINIA	12507	2540	1.07	35.80	47.03	0.56
174715	KENTUCKY	13080	2620	6.40	38.50	51.60	0.60
220428	ALABAMA	14170	2000	4.55	34.23	58.38	1.59
AVE 3	MONTANA	9699	2315	21.60	32.00	43.40	1.10
177516	COLORADO	11730	2420	6.40	36.10	50.10	0.70
179379	NORTH DAKOTA	6260	2235	43.10	27.40	24.80	0.70
AVE 4	MONTANA	9689	2125	22.10	31.25	43.70	0.20
AVE 2	MONTANA	7152	2373	33.36	29.73	31.53	0.53

223560	NEW MEXICO	12745	2800	2.22	36.41	48.69	0.66
180080	NORTH DAKOTA	6060	2410	44.70	25.50	25.20	0.40

A statistical parameter was introduced to quantitatively assess the error and accuracy in testing each of the models. This error function is presented in Equation 4.5.

$$\chi = \frac{\sum^{n} \left| \frac{X_{predicted} - X_{actual}}{X_{actual}} \right|}{n} \qquad (4.5)$$

Where N is the number of data sets used in querying the model, $X_{predicted}$ represents the predicted value group, and X_{actual} represents the actual value group. From Equation 4.5, it can be seen that the lower the value of χ is, the closer $X_{predicted}$ and X_{actual} are. The interpretation of this parameter is that it provides the degree of confidence one tabulated set of data is similar (or different) to another set. The threshold for χ is strongly dependent on the absolute values of the data. In this study, comparison results with χ value less than 0.3 were considered to be acceptable results for the index Fs. For Ti the threshold for χ was 0.03.

4.3 Fs Modeling results

To build and test the ANN model for Fs, 4,528 coals from the U.S. Geological database were use to relate the Fs index. These coals were all the applicable bituminous and sub-bituminous coals included in the database. These sets of values were used as model inputs, and calculated values of Fs were used as model training targets. In

training and testing the model for Fs, 100 coals were randomly selected from the 4,582 coals as the test and comparing group, and the rest 4,428 coals were used to build the neurofuzzy model. The training took approximately two hours to successfully generate a neurofuzzy model. With this model, the 100 testing coals data were interrogated into the model. Using the "query command" to run the neurofuzzy model, 100 Fs values were predicted. Figure 4.2 shows the comparison between the predicted and actual Fs.

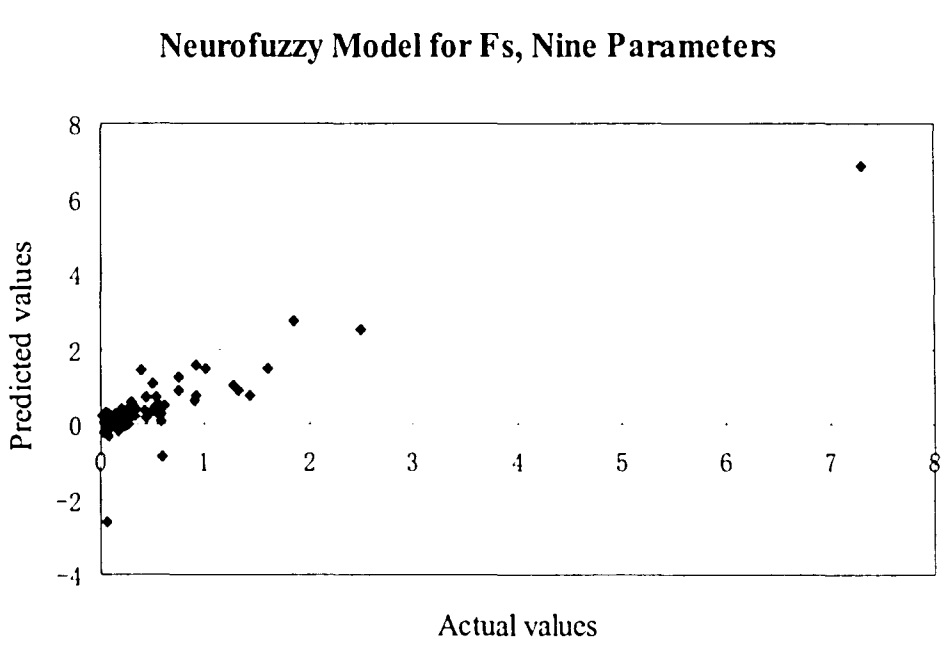

Figure 4.2: Comparisons Between Predicted Values and Actual Values for Neurofuzzy model, Nine Inputs

The error for this model was:

$\chi_{Fuzzy} = 1.54$

As it can be seen, the error function exceeded 0.3 and the comparison plot was quite scattered. This model was deemed not accurate. Therefore a pre-processing was applied to the model inputs and targets data to improve the model performance. This pre-processing of the data was applied to the variables before feeding them to the ANN for training. A standardization of the data was applied where the data were transformed to achieve zero mean and unity standard deviation according to:

$$X_1 = \frac{X - \overline{X}}{\sigma} \tag{4.6}$$

The data were then scaled to fit in the [0,1] range following Equation 4.7:

$$X_2 = \frac{X_1 - \min(X_1)}{\max(X_1) - \min(X_1)} \tag{4.7}$$

Where X is the original data vector, X_1 is the auto-scaled data vector, X_2 is the linear scaled data vector, $\overline{X}$ is the average of all the data in the vector, and σ is the standard deviation of all the data in the input vector. Once the model was built and queried Fs values were predicted, they were transferred back to the original Fs values by reversing the pre-processing steps.

A new neurofuzzy model was then built, using 3,527 sets of only bituminous coals, and coals with Fs values less than 5. All of the 3,527 Fs values were manipulated through the pre-processing step into normalized Fs values before being fed to ANN model. Similarly, 100 random coals were used to query in the model, while the rest 3,427 coals were used to train the neurofuzzy model. Figure 4.3 displays the comparison between model predicted values and actual values for this model.

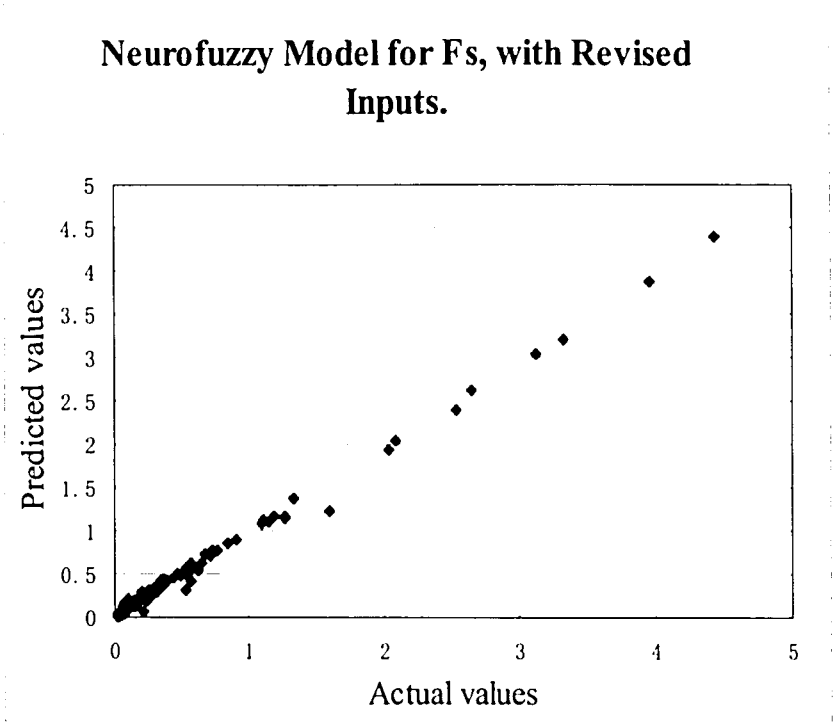

Figure 4.3: Comparison Between Predicted Values and Actual Values for Neurofuzzy Model, Nine Inputs, Pre-processed Fs Values

The error for this model was:

χ_{Fuzzy} = 0.158

From the error function value we can see the new model had a considerable improvement over the previous model.

4.4 Ti Modeling Results

For the other slagging index, ash fusion temperature or Ti, a similar testing

procedure (using the linear and non-linear mathematical models), was performed. Data from the U.S. Geological Survey Report were used, as well as MATLAB 7 solution schemes to solve for the coefficients in the equations and calculate the predicted Ti.

First, the linear Ti model was tested. A 4,501 random set of coal data from the U.S. Geological Survey Report was selected as the model training data set. Another set of 100 coals data was randomly chosen to query the coefficients in the model. The predicted and actual Ti temperatures are shown as in Figure 4.4.

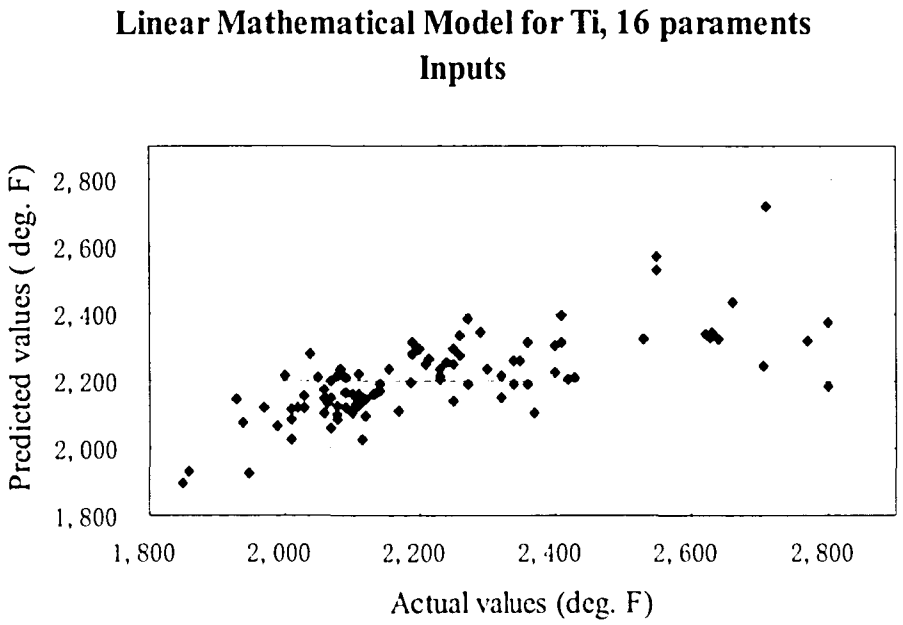

Figure 4.4: Comparisons Between Predicted Values and Actual Values for Linear Model for Ti, Sixteen Inputs

The error for this model was:

χ_{linear}=0.0492

Similarly, using the same data set as for the linear model, the non-linear relationship was tested. The identical test set of 100 coals was used for comparison. The predicted and actual fusion temperatures are shown as in Figure 4.5.

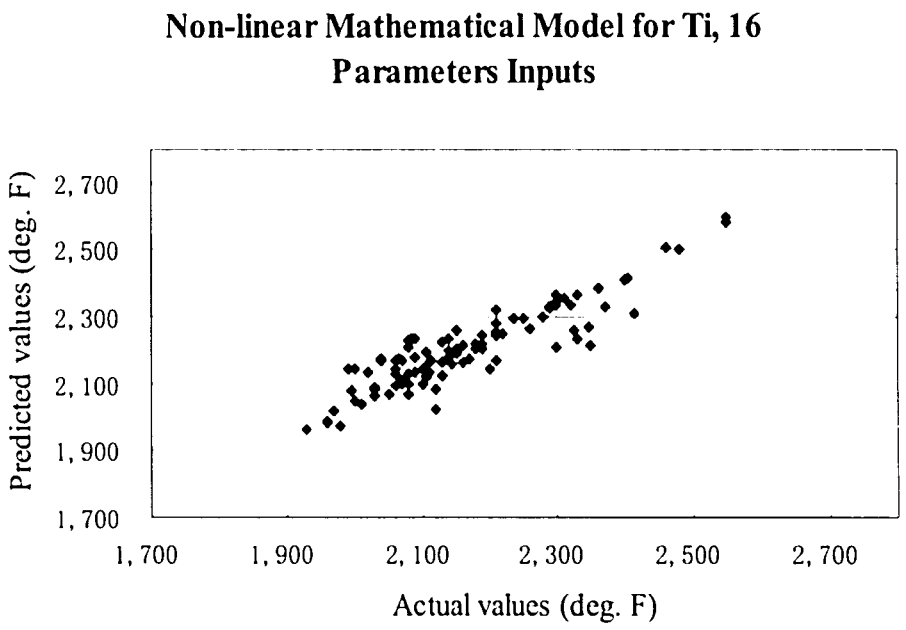

Figure 4.5: Comparisons Between Predicted Values and Actual Values for Non-linear Model for Ti, Sixteen Inputs

The error for this model was:

$\chi_{non-linear}$=0.0264

According to the value of the corresponding errors, it can be concluded that the non-linear regression provides a better predicting for Ti over the linear regression model.

Chapter5: Experimental Results

5.1 Results for Simulated Samples

Operation of the LIBS system on a coal sample results in light spectra containing different intensities at defined wavelengths. These wavelengths and intensities are used to determine the actual concentrations of the different elements of interest present in the coal sample. The determination of the coal chemical analysis using the LIBS spectra strongly depends on the LIBS ability to differentiate the elemental composition in the LIBS intensity vs. wavelength trace. Following is an example of a typical data plot from the LIBS measurements made on one pulverized coal sample. The starting step in obtaining information from IBS spectra is identifying the peaks in the spectra. A small section of the LIBS spectra is shown in Figure 5.1. The useful peaks in this spectrum were identified using published lists of atomic emission lines. After the peaks are identified, the areas under the spectral peaks for different elements are quantified measured. Using Figure 5.1 as an example, if a different coal sample is analyzed that has more aluminum relative to silica, its spectra would have a relatively larger area under the aluminum peak as compared to the silica peak.

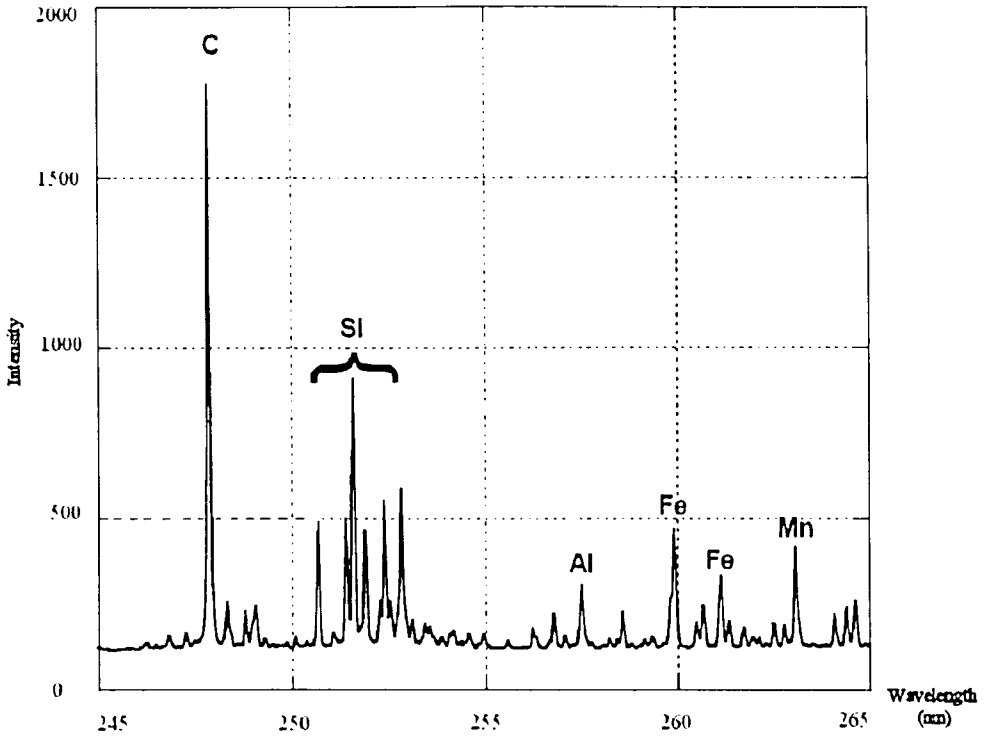

Figure 5.1: Sample LIBS Spectrum from Coal Sample (Elemental Concentrations in Sample: C = 75.13%, Si = 2.3%, Al = 1.6%, Fe = 1.1%, Mn= 77 ppm)

5.1.1 Molar Ratio Calculation

To validate the feasibility of the LIBS technique to determine concentrations of elemental species in coal samples, synthetic samples were first prepared containing the elements of interest. The elements chosen were those that are related to the slagging indices Fs and Ti. From the definitions of these two indices and their analyses from previous chapters, the elements of interest include: C, H, O, S, and N, as well as, Si, Al, Ti, Fe, Ca, Mg, Na, and K.

The plasma spark emission from the interaction with the sample was investigated with the setup that includes the Echelle spectrometer, the Acton spectrometer and the photodiodes. The data collected from this system was analyzed with a simple integration method to produce relevant signals, proportional to the amount of the elements in the sample. The signals produced from the experiments were then compared to the actual sample compositions (indicated by standardized laboratory analysis) by comparing the LIBS element to carbon signal ratio to the same molar ratio of element to carbon. It should be mentioned that the LIBS measurements produce elemental results that are very distinct that the comparative analysis determined under standardized ASTM methods, which report the coal ultimate analysis and ash mineral composition. The standardized ash mineral analysis provides mineral composition on an oxidized basis (due to the nature of the technique), in contrast to the LIBS results, which are on an "as-is" basis. For this reason, a procedure was developed to convert coal standardized laboratory analysis for appropriate element to C molar ratio for comparison to the LIBS data ratios.

The coal standardized laboratory analysis includes moisture, C, H, N, O, S, Cl, percent ash, and ash composition. Table 5.1 shows these parameters and the variables assigned to these parameters for the calculations.

Table 5.1 Coal Standard Components

Parameter	Variable for Reported Value

Moisture		x_M
C		x_C
H		x_H
N		x_N
O		x_O
S		x_S
Cl		x_{Cl}
Ash		x_A
Ash Constituents	SiO_2	x_{A_SiO2}
	Al_2O_3	x_{A_Al2O3}
	TiO_2	x_{A_TiO2}
	Fe_2O_3	x_{A_Fe2O3}
	CaO	x_{A_CaO}
	MgO	x_{A_MgO}
	Na_2O	xA_{Na2O}
	K_2O	xA_{K2O}
	SO_3	xA_{SO3}

The first step was to convert the compositions to a dry basis and normalize the compositions to percentage. The concentration data fall in to two groups. In the first group,

$$x_M + x_C + x_H + x_O + x_S + x_{Cl} + x_A \cong 100\% \qquad (5.1)$$

In the second group, the sum in Equation 5.2 is found to be significantly greater than 100 percent. The C, H, O, S, Cl, and ash compositions were provided on a dry basis, thus,

$$x_C + x_H + x_O + x_S + x_{Cl} + x_A \cong 100\% \qquad (5.2)$$

Furthermore, x_H and $x_O$were assumed to be the amounts of hydrogen and oxygen portion presented in the sample not associated with free moisture. With this assumption, a dry normalized composition was determined for both cases by normalizing the C, H, O,

S, Cl, and ash concentrations to 100 percent:

$$x_i' = 100 \times \frac{x_i}{x_C + x_H + x_O + x_S + x_A} \qquad (5.3)$$

Where: i = C, H, O, S, Cl, and A. The prime mark indicates a dry normalized composition by weight.

The metal compositions of the ash were also normalized according to:

$$x_{A\_i}' = 100 \times \frac{x_{A\_i}}{\sum_j x_{A\_j}} \qquad (5.4)$$

Where i and j = the ash constituents in Table 5.1

Then, dry normalized compositions were converted to elemental weight percent compositions (f_i, where i = C, H, N, O, S, Cl, Si, Al, Ti, Fe, Ca, Mg, Na, K, and Na). In this step, the compounds are split into their individual elements and the elements are added from each compound. Since C, H, N, and Cl are not contained in any of the compounds, their weight percents were simply carried over:

$$f_j = x_j' \qquad (5.5)$$

Where j = C, H, N, and Cl.

In the analysis, O is listed as oxygen and oxygen in the metal oxides in the ash. The overall fraction of oxygen, f_O, is then found by:

$$f_O = x_O' + x_A' \sum_j \frac{n_j MW_O}{MW_{Oxide\_j}} x_{A\_j}' \qquad (5.6)$$

Where the chemical formula of oxide j in the ash is $M_{m_j}O_{n_j}$, n_j is the number of oxygen in oxide j, MW_O is the molecular weight of oxygen, and MW_{Oxide_j} is the molecular weight of oxide j.

Similarly, S is presented in the ultimate analysis and the ash analysis. These S values can be combined to give the total sulphur content in the coal:

$$f_S = x_S' + x_A' \frac{MW_S}{MW_{SO_3}} x_{A\_SO3}' \qquad (5.7)$$

The metals in the coal are reported as oxides in the coal. Their weight percentage can be found from the ash concentration, the percentage of oxide in the ash and the weight fraction of the metal in the oxides (x_{A_j}). This is illustrated in the following equation:

$$f_j = x_A' \frac{m_j MW_j}{MW_{Oxide\_j}} x_{A\_j} \qquad (5.8)$$

Where m_j = number of metals in chemical formula and MW_j = molecular weight of metal.

The weight percents of individual elements, f_j, were then converted to moles, F_j, by dividing by the atomic weight of the elements, using:

$$F_j = \frac{f_j}{MW_j} \qquad (5.9)$$

Finally, the mole amounts were then normalized to a total of 100 by:

$$F_j' = 100 \times \frac{F_j}{\sum_i F_i} \qquad (5.10)$$

Using these molar concentration values, each of the desired molar ratios of the individual elements to carbon was then calculated.

5.1.2 Simulated Coal Experiments Performing

The experiments performed in this study had three components associated to them: sample preparation, spectra data collection or measurements and data analysis. The following sections reports on each of these steps:

For the sampling of simulated coal species, sample preparation consisted first of selecting the appropriate chemical compounds to be used to simulate the elements of interest in the coal. These compounds were then mixed and mount as mixed samples for LIBS analysis.

The base mixture used in the synthetic coal testing was anthracene ($C_{14}H_{10}$). Anthracene was selected as the base material because it is available as a coarse powder which can be crushed, also due to its H/C ratio, which is similar to that of real coal samples. The compounds selected to bring the metal elements into the base were based on their chemical stability and ease to disperse into anthracene. For example, regarding chemical stability, $CaCO_3$ was selected to introduce Ca into the base over selecting CaO because of the reactivity of CaO with CO_2 and H_2O in the atmosphere. Most of the metal

compounds were available as fine powders which allowed them to be evenly dispersed into the anthracene. The salts of Na and K were easy to crush into a fine powder and thus dispersed into the base too. A list of the compound names, formula, and catalog numbers (for purchasing purpose only) of these compounds is given in Table 5.2.

Table 5.2: Compounds used to introduce metals to carbon-hydrogen base.

		Compound Used in Surrogate		
Metal	Oxide	Name	Formula	Catalog No.
Si	SiO_2	silica	SiO_2	89709
Al	Al_2O_3	alumina	Al_2O_3	12553
Ti	TiO_2	titanium (IV) oxide	TiO_2	43047
Fe	Fe_2O_3	iron (III) oxide	Fe_2O_3	12375
Ca	CaO	calcium carbonate	$CaCO_3$	36337
Mg	MgO	magnesium carbonate tetrahydrate	$4MgCO_3.Mg(OH)_2.4H_2O$	33333
K	K_2O	potassium bromide	KBr	12612
Na	Na_2O	sodium chloride	NaCl	12314

Before the preparation of the actual samples, target compositions were determined to make sure that the element to carbon ratios would cover the range of real compositions of coal samples. This typical range of coal compositions was determined from the chemical analysis report of the coal samples (refer to Table 5.3). The samples for the LIBS measurements, weighed about 5g each, and were prepared by first weighing out the compounds to the nearest 0.0001g. The additives to the base were placed in a mortar and combined with a pestle to produce a uniform mixture. A small amount of anthracene was then added to the mixture with the additives.

Table 5.3 Chemical Analysis Report and Calculated Slagging Indices of Coal Samples

	BITUMINOUS COALS											
CODE SAMPLE	*BIT-HAT*	*BIT-HAR*	*BIT-PLE*	*BIT-LOG*	*Russian*	*Oxbow/Arch*	*Cerrejon*	*Drummond*	*Calenturitas*	*DECS-2 Randolph, IL*	*DECS-17 Emery,UT*	*DECS-18 Union, KY*
SUPPLIER	Allegheny Energy	Allegheny Energy	Allegheny Energy	NRG	Constellation	Dominion	Dominion	Dominion	Dominion	Coal Bank PSU	Coal Bank PSU	Coal Bank PSU
PLANT	Hatfield Ferry St.	Harrison St.	Pleasant St.	Logan St.	Brandon Shores St.	Brayton Point St.	Brayton Point St.	Brayton Point St.	Brayton Point St.			
DATE	12/22/2005	12/23/2005	12/24/2005	4/7/2006	2/17/2006	2/28/2006	6/13/2005	2/26/2006	3/24/2006	5/16/2006	5/16/2006	5/16/2006
PROXIMATE ANALYSIS												
INHERENT MOISTURE, PCT WT	6.68	0.94	1.48	1.73	11.77	5.56	10.92	11.90	13.51	10.43	3.74	6.61
ASH, PCT WT	8.64	14.21	9.43	10.52	11.81	9.37	7.35	3.90	6.59	14.47	6.32	11.42
ASH, PCT WT, DRY	9.26	14.34	9.57	10.71	13.39	9.92	8.25	4.42	7.62	16.16	6.57	12.25
VOLATILE MATTER, PCT WT	34.67	38.61	41.67	32.75	28.07	39.17	33.62	35.77	35.38	34.16	45.00	38.38
VOLATILE MATTER, PCT WT, DRY	37.36	38.98	42.30	33.33	31.82	41.48	37.73	40.80	40.91	38.14	46.75	41.18
SULPHUR, PCT WT	2.26	3.69	4.77	1.06	0.58	0.48	0.64	0.46	0.47	4.05	0.42	3.92
SULPHUR, PCT WT, DRY	2.42	3.72	4.84	1.08	0.65	0.50	0.72	0.52	0.54	4.52	0.44	4.21
FIXED CARBON, PCT WT	49.81	46.24	47.42	54.99	48.34	45.90	48.11	48.44	44.52	40.93	44.93	43.40
FIXED CARBON, PCT WT, DRY	53.36	46.66	48.13	55.96	54.79	48.60	54.00	54.98	51.47	45.70	46.68	46.57
GROSS CALORIFIC VALUE, BTU/LB	12,773	12,929	13,205	13,207	11,431	12,457	11,842	11,633	10,954	14,061	14,363	14,226
LB SO2/MMBTU							1.06					
HARDGROVE GRINDABILITY INDEX												
MINERAL ANALYSIS FOR ASH (BY WT)												
SILICA, SiO2	46.60	44.65	38.10	52.63	54.86	58.43	60.51	46.14	60.19	49.20	47.60	41.20
ALUMINA, Al2O3	21.40	18.70	18.60	28.08	27.98	23.64	20.06	20.75	20.40	19.10	9.23	15.60
TITANIA, TiO2	1.02	0.92	0.86	1.53	1.34	0.90	0.91	0.81	0.88	0.89	0.76	0.75
FERRIC OXIDE, Fe2O3	18.17	18.89	30.57	6.41	3.84	4.51	8.71	8.32	6.55	20.40	7.92	22.00
LIME, CaO	3.31	7.29	2.67	2.15	2.01	3.25	2.47	6.05	2.17	5.18	4.80	8.06
MAGNESIA, MgO	0.77	1.11	0.62	0.75	1.37	1.05	2.14	1.75	1.68	0.82	1.96	0.70
SODIUM OXIDE, Na2O	0.53	0.62	0.40	0.22	0.35	1.00	0.52	1.56	0.44	0.71	6.36	0.66
POTASSIUM OXIDE, K2O	2.62	1.07	3.32	3.17	3.21	1.33	2.08	2.94	1.58	1.87	0.49	1.89
SULFUR TRIOXIDE, SO3	2.61	3.88	2.07	1.96	1.83	1.77	2.09	8.81	3.31	1.60	10.90	9.40
FUSION TEMPERATURE (DEG. F, RED.)												
INITIAL DEFORMATION TEMP, IT	2,120	2,040	2,000	2,700	2,700	2,480	2,226	2,300	2,480	1,900	1,800	1,755
SOFTENING TEMP, (H=W) ST	2,187	2,100	2,040	2,700	2,700	2,520	2,337	2,360	2,520	2,035	1,900	1,900
HEMISPHERICAL TEMP, (H=1/2 W), HT	2,247	2,180	2,080	2,700	2,700	2,600	2,463	2,400	2,600	2,100	1,965	2,000
FLUID TEMP, FT	2,303	2,290	2,100	2,700	2,700	2,700	2,549	2,510	2,700	2,160	2,020	2,040
ULTIMATE ANALYSIS (BY WT)												
TOTAL MOISTURE	6.68	0.94	1.48	1.73	11.77	5.56	10.92	11.9	13.51	10.43	3.74	6.61
CARBON	72.56	72.79	74.08	76.84	65.27	70.07	66.15	68.07	64.12	65.49	76.25	69.39
HYDROGEN	4.83	4.97	5.07	4.97	4.11	4.92	4.65	4.57	4.27	4.56	5.80	5.09
NITROGEN	1.35	1.23	1.20	1.45	0.07	1.55	1.21	1.37	1.31	1.11	1.29	1.26
OXYGEN	3.61	2.11	3.92	3.30	5.17	8.01	9.06	9.72	9.72	8.16	9.65	7.80
SULPHUR	2.26	3.69	4.77	1.06	0.58	0.48	0.64	0.46	0.47	4.52	0.44	4.21
ASH	8.64	14.21	9.43	10.52	11.61	9.37	7.35	3.90	6.59	16.16	6.57	12.25
CHLORINE	0.06	0.06	0.05	0.13	0.07	0.04	0.03	0.01	0.01	0.12	0.11	0.16
MERCURY (PPM), dry basis				0.24								
COAL INDICES												
ASH DESCRIPTOR												
IRON OXIDE OF ASH	18.17	18.89	30.57	6.41	3.84	4.51	8.71	8.32	6.55	20.40	7.92	22.00
LBS IRON PER MBTU	1.23	2.08	2.18	0.51	0.40	0.34	0.54	0.28	0.38	2.10	0.35	1.77
SILICA RATIO	67.68	62.07	52.95	84.97	88.37	86.90	81.86	74.11	85.27	65.08	78.43	57.24
R_{SR}	0.76	0.71	0.63	0.90	0.93	0.91	0.86	0.82	0.90	0.73	0.82	0.65
DOLOMITE RATIO	0.16	0.29	0.09	0.23	0.31	0.39	0.29	0.38	0.31	0.21	0.31	0.26
ASH VISCOSITY, T_{250} OF ASH, DEG. F	NA	NA	NA	NA	NA	NA	NA	NA	NA	NA	NA	NA
SLAGGING PROPENSITY												
BASE/ACID RATIO	0.37	0.45	0.65	0.15	0.13	0.13	0.20	0.30	0.15	0.42	0.37	0.58
SLAGGING FACTOR, Fs	0.89	1.68	3.16	0.17	0.08	0.07	0.14	0.16	0.08	1.89	0.16	2.44
IRON/CALCIUM RATIO	5.49	2.59	11.45	2.98	1.91	1.39	3.53	1.38	3.02	3.94	1.65	2.72
SILICA/ALUMINA RATIO	2.18	2.39	2.05	1.87	1.96	2.47	3.02	2.22	2.95	2.58	5.16	2.64
SLAGGING FACTOR, DEG F	2,145	2,068	2,016	2,700	2,700	2,504	2,273	2,320	2,504	1,940	1,833	1,804
FOULING PROPENSITY												
SODIUM CONTENT OF ASH	0.53	0.62	0.40	0.22	0.35	1.00	0.52	1.56	0.44	0.71	6.36	0.66
SODIUM CONTENT OF ASH	0.53	0.62	0.40	0.22	0.35	1.00	0.52	1.56	0.44	0.71	6.36	0.66
SODIUM EQUIVALENT	0.21	0.19	0.25	0.25	0.33	0.19	0.18	0.15	0.11	0.31	0.44	0.23
CHLORINE CONTENT OF ASH	0.06	0.05	0.05	0.13	0.07	0.04	0.03	0.01	0.01	0.12	0.11	0.16
FOULING FACTOR, Fx	1.07	1.37	0.98	1.08	1.31	1.36	1.09	1.13	1.02	1.56	3.11	1.23
FOULING FACTOR, Fy	0.20	0.28	0.26	0.03	0.04	0.13	0.10	0.48	0.07	0.30	2.38	0.38

Continued…

Table 5.3 Chemical Analysis Report and Calculated Slagging Indices of Coal Samples, Continued

	LIGNITIC COALS									
CODE SAMPLE	*DECS-1 Freestone TX*	*DECS-9 Bighorn, MT*	*100% Western*	*85/15 % Western/Eastern*	*Adaro*					
SUPPLIER	Coal Bank PSU	Coal Bank PSU	DTE-Energy	DTE-Energy	PSE&G					
PLANT			St. Clair St.	St. Clair St.	Bridgeport St.					
DATE	5/16/2006	5/16/2006	1/20/2006	1/18/2006	1/21/2006					
PROXIMATE ANALYSIS										
INHERENT MOISTURE, PCT WT	30.00	24.68	17.21	16.95	14.50					
ASH, PCT WT	11.07	4.80	5.04	5.47	1.10					
ASH, PCT WT, DRY	15.81	6.37	6.09	6.59	1.29					
VOLATILE MATTER, PCT WT	33.18	33.46	40.04	34.65	37.80					
VOLATILE MATTER, PCT WT, DRY	47.40	44.43	48.36	41.27	44.21					
SULPHUR, PCT WT	0.69	0.31	0.33	0.45	0.09					
SULPHUR, PCT WT, DRY	0.98	0.41	0.40	0.54	0.11					
FIXED CARBON, PCT WT	25.75	37.06	37.71	42.93	34.90					
FIXED CARBON, PCT WT, DRY	36.79	49.20	45.55	51.69	40.82					
GROSS CALORIFIC VALUE, BTU/LB	12,812	12,809	10,215	10,255	9,211					
LB SO2/MMBTU										
HARDGROVE GRINDABILITY INDEX										
ORDINAL ANALYSIS FOR ASH (BY WT)										
SILICA, SiO2	45.60	36.20	30.56	33.03	34.21					
ALUMINA, Al2O3	17.00	18.10	14.60	14.79	17.05					
TITANIA, TiO2	1.26	1.20	1.06	1.05	0.69					
FERRIC OXIDE, Fe2O3	4.18	4.90	4.07	5.05	17.59					
LIME, CaO	5.50	13.50	23.63	13.23	13.00					
MAGNESIA, MgO	2.68	4.52	3.06	2.82	3.96					
SODIUM OXIDE, Na2O	0.42	5.55	3.92	3.88	0.21					
POTASSIUM OXIDE, K2O	0.60	1.01	0.39	2.81	0.99					
SULFUR TRIOXIDE, SO3	12.70	13.40	15.60	20.31	11.84					
FUSION TEMPERATURE (DEG. F, REDUCING)										
INITIAL DEFORMATION TEMP, IT	1,840	1,910	2,090	2,000	2,138					
SOFTENING TEMP, (H=W) ST	2,000	1,990	2,120	2,030	2,192					
HEMISPHERICAL TEMP, (H=1/2 W), HT	2,060	2,040	2,140	2,090	2,210					
FLUID TEMP, FT	2,100	2,090	2,160	2,120	2,318					
ULTIMATE ANALYSIS (BY WT)										
TOTAL MOISTURE	30	24.68	17.21	16.95						
CARBON	62.53	70.73	60.99	61.61	72.00					
HYDROGEN	4.75	4.85	4.03	3.99	4.79					
NITROGEN	1.23	0.84	0.75	0.78	0.84					
OXYGEN	14.69	16.80	11.64	10.73	20.73					
SULPHUR	0.99	0.41	0.33	0.45	0.12					
ASH	15.81	6.37	5.04	5.47						
CHLORINE	0.11	0.09	0.01	0.02						
MERCURY (PPM), dry basis					0.03					
						COAL ASH INDICES				
COAL INDICES						LOW	MED		SEVERE	
ASH DESCRIPTOR										
IRON OXIDE OF ASH	4.18	4.90	4.07	5.05	17.59	3-8	8-15	8-15	15-23	
LBS IRON PER MBTU	0.36	0.18	0.20	0.27	0.21	Low ←			→ High	
SILICA RATIO	78.67	61.23	49.82	61.02	49.75	72-80	65-72	65-72	50-65	Applies for coals ashes that do not contain sodium at above 2.5% or calcium at above 7.5%.
R_{250}	0.87	0.75	0.62	0.72	0.63	Low ←			→ High	
DOLOMITE RATIO	0.61	0.61	0.76	0.56	0.47	Low ←			→ High	
ASH VISCOSITY, T_{250} OF ASH, DEG. F	NA	NA	NA	NA	NA	>1,302	1,399-1,145	1,236-1,121	<1,204	
SLAGGING PROPENSITY										
BASE/ACID RATIO	0.21	0.53	0.76	0.57	0.09	<0.5	0.5-1.0	1.0-1.75	>1.75	For lignitic ash: %CaO + % MgO > %Fe_2O_3 (ACIDIC ASHES)
SLAGGING FACTOR, Fs	0.21	0.22	0.30	0.31	0.08	<0.6	0.6-2.0	2.0-2.6	>2.6	For bituminous ash: %CaO + %MgO < %Fe_2O_3 (ALKALINE ASHES)
IRON/CALCIUM RATIO	0.76	0.36	0.17	0.36	1.35	<0.31 OR >3.0 ←		0.31-3.0	→	
SILICA/ALUMINA RATIO	2.68	2.00	2.09	2.23	2.01	Low ←			→ High	
SLAGGING FACTOR, DEG F	1,864	1,936	2,100	2,018	2,152	>2,449	2,250-2,449	2,100-2,250	<2,100	
FOULING PROPENSITY										
SODIUM CONTENT OF ASH	0.42	5.55	3.92	3.88	0.21	<2.0	2.0-6.0	6.0-8.0	>8.0	For lignitic ash: %CaO + % MgO > %Fe2O3 (ACIDIC ASHES)
SODIUM CONTENT OF ASH	0.42	5.55	3.92	3.88	0.21	<0.5	0.5-1.0	1.0-2.5	>2.5	For bituminous ash: %CaO + %MgO < %Fe_2O_3 (ALKALINE ASHES)
SODIUM EQUIVALENT	0.13	0.40	0.25	0.36	0.01	<0.3	0.3-0.45	0.45-0.60	>0.6	For bituminous ash: %CaO + %MgO < %Fe_2O_3 (ALKALINE ASHES)
CHLORINE CONTENT OF ASH	0.11	0.09	0.01	0.02	0.00	<0.3	0.3-0.5	0.3-0.5	>0.5	British coal ashes
FOULING FACTOR, Fx	1.41	2.65	1.90	2.01	0.30	Low ←			→ High	Low-rank Western U.S. subbituminous coal ashes
FOULING FACTOR, Fy	0.09	2.95	2.98	2.21	0.14	<0.2	0.2-0.5	0.5-1.0	>1.0	For bituminous ash: %CaO + %MgO < %Fe_2O_3 (ALKALINE ASHES)

The remaining anthracene was then added to the mortar and mixed. Samples of lower concentrations were prepared by diluting initial samples with additional anthracene. After the stimulated samples of anthracene mixtures were prepared, the same sample preparing procedures as described in Chapter 3 were applied too. Afterwards, the containers with simulated samples on the bottom were placed in the chamber and ready for tests.

The experimental setup parameters were held constant among the measurements performed on the samples. i.e., the chamber pressure were at 21 inches Hg all the time, time intervals between laser shots were always approximate four seconds and detectors angles in the chamber remained still for all the samples. The metals, except K, were determined from spectral lines observed in the spectra collected with the Echelle spectrometer. The sulphur in the samples was investigated using the spectra collected with the Acton spectrometer, while the H, O, and K were determined using time traces collected with the photodiodes. For the synthetic coal samples, for each powder sample prepared, spectral data were collected from at least three samples to allow error calculations to be performed. For each LIBS test, fifty spectra were accumulated and saved as a single spectrum for later analysis.

The first step in the data analysis for the collected spectra consisted of insuring that the correct elements were assigned to the observed spectral lines and that observed lines were not the result of overlapping lines from different species. To insure this, spectra collected from the synthetic samples containing no additions and containing

single element additions were compared, as well as those of the real coal samples. Furthermore, only strong lines listed in the Kurucz spectral line database were considered. Kurucz spectral line database stores emission line wavelengths for different elements stretching from the vacuum ultraviolet through to the near infrared (approximate 200 nm to 780 nm). Table 5.4 shows a part of the Kurucz spectral line database.

Table 5.4 Partial Data from Kurucz Spectral Line Database

Wl / nm vac<200nm <air	log_gf	Elem.Element (Code)(Name)	E lowerlev. / cm^(-1)	J lowe r	E upper lev. / cm^(-1)	J Ref. upper
200.0525	-3.348	14.00 Si I	15394.370	0.0	65365.050	1.0 K
201.8974	-1.100	15.00 P I	18748.010	1.5	68262.151	2.5 KP
202.5824	-0.600	12.00 Mg I	0.000	0.0	49346.729	.0 GUES
206.5776	-0.322	5.02 B III	0.000	0.5	48392.500	1.5 LN
207.6236	-3.890	13.00 Al I	112.061	1.5	48260.794	2.5 NBS
208.9556	-0.743	5.00 B I	15.150	1.5	47857.000	2.5 BRO
367.1612	-1.950	3.00 Li I	14903.654	0.5	42131.891	1.5 LN
421.3001	-2.650	11.00 Na I	16956.172	0.5	40685.535	1.5 GUES
475.3930	-2.970	19.00 K I	13042.876	1.5	34072.220	0.5 NBS

For the spectral lines associated with specific elements, the line intensities were determined by integration. The integration was performed by simply summing the intensities over the wavelength range of the signal peak. For the spectra collected with the Echelle spectrometer, the background intensities were very low compared to the spectral line intensities. In this case, a background correction was not made. For the spectra collected with the Acton spectrometer, the background was determined by averaging the intensities surrounding the spectral line of interest. This background intensity was corrected for the number of points in the spectral line wavelength range and then was subtracted from the calculated line intensity.

The photodiode signals were determined by subtracting an exponential background from the element traces and then integrated over a set time range. This time range was selected to eliminate the initial plasma spark, and the spectral line emissions were expected to be minimal. Again, the integration was performed by adding up the intensities within the set time range. The exponential background signal was derived from a photodiode trace collected at 838 nm. [5.1]

5.1.3 Experimental Results for Simulated Samples

The correlation between the measured line intensities (with respect to C) and concentrations of the elements (with respect to C) from the synthetic coal samples were recorded and plotted. These plots contained comparisons of the intensity ratios of a spectral line from the element of interest to the C 247 nm line vs. the reported molar ratio of the element to carbon. The resulting "calibration" curves are shown in Figures 5.2 to Figure 5.11.

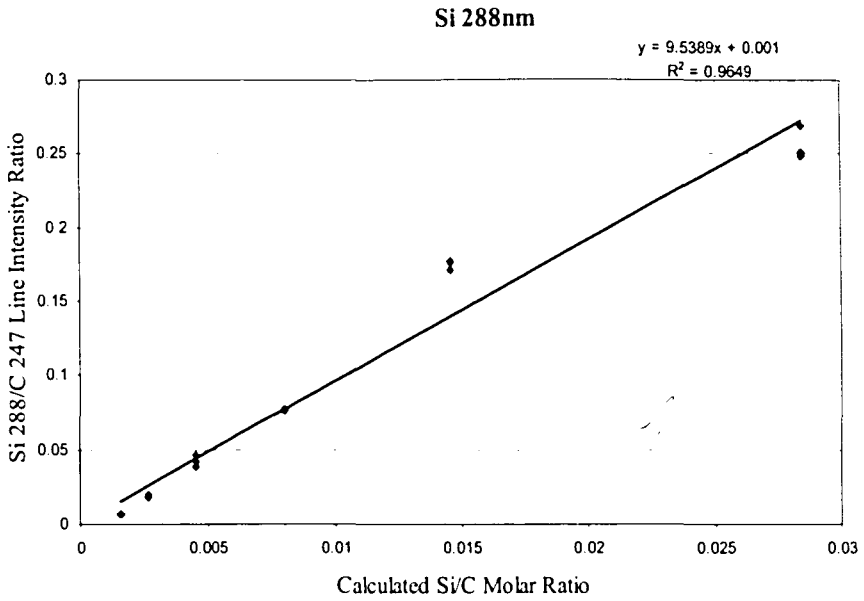

Figure 5.2: Calibration Plot for Si Emission Line

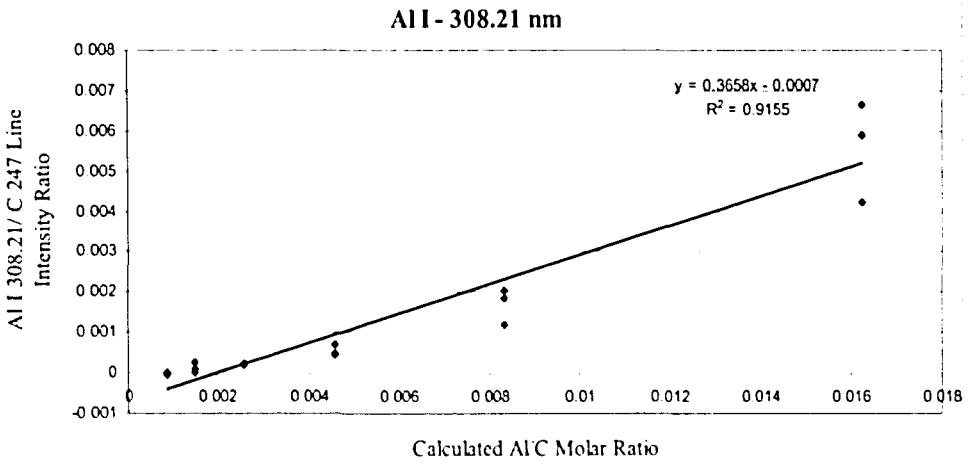

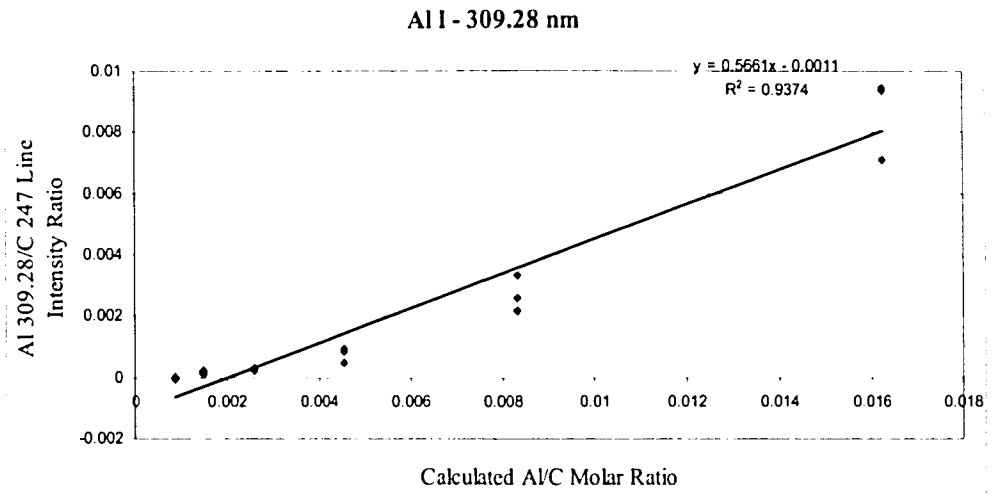

Figure 5.3: Calibration Plots for Al Emission Lines

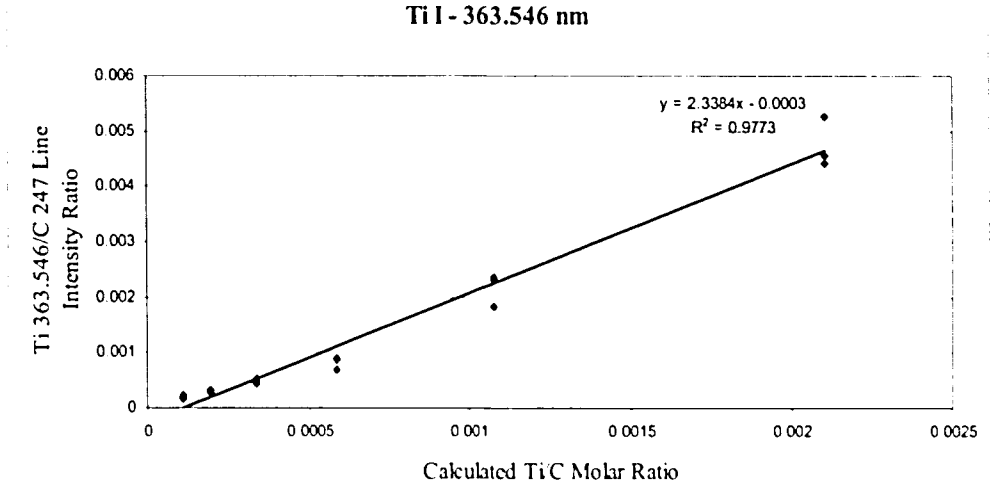

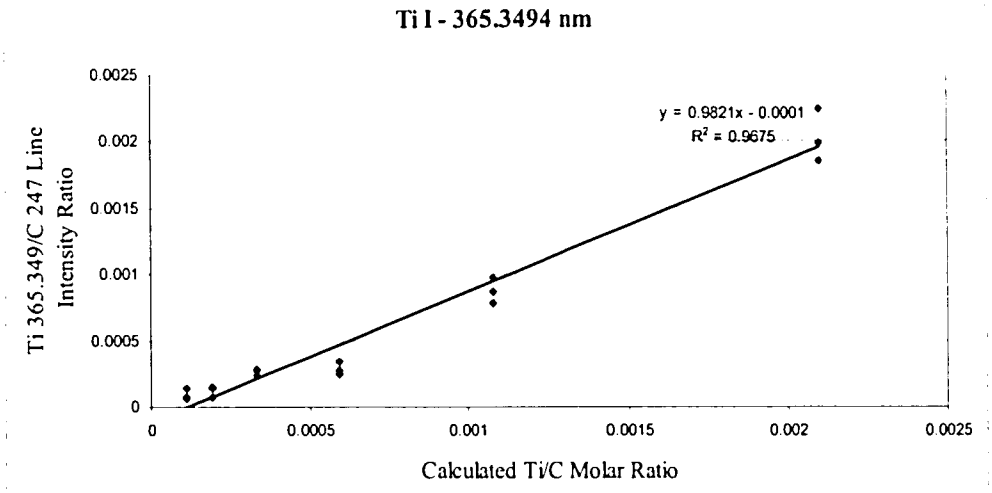

Figure 5.4: Calibration Plots for Ti Emission Lines

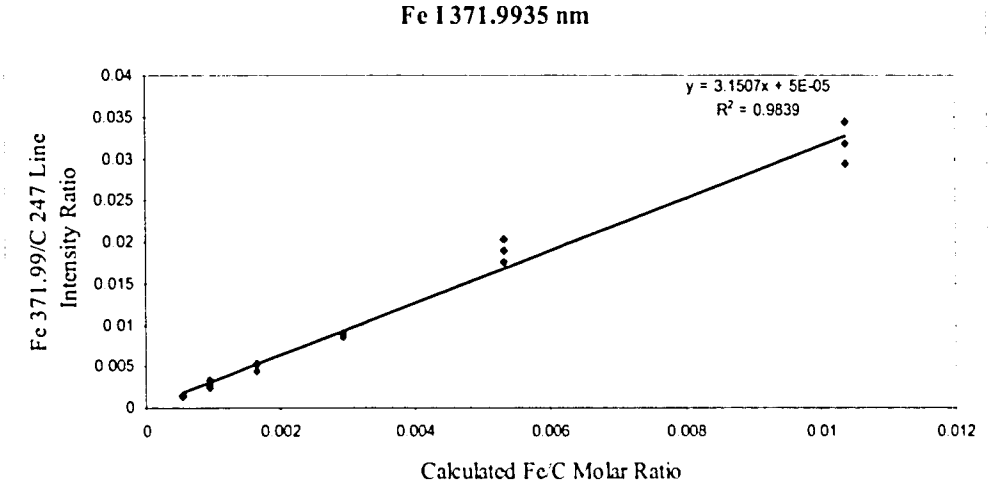

Figure 5.5: Calibration Plot for Fe Emission Line

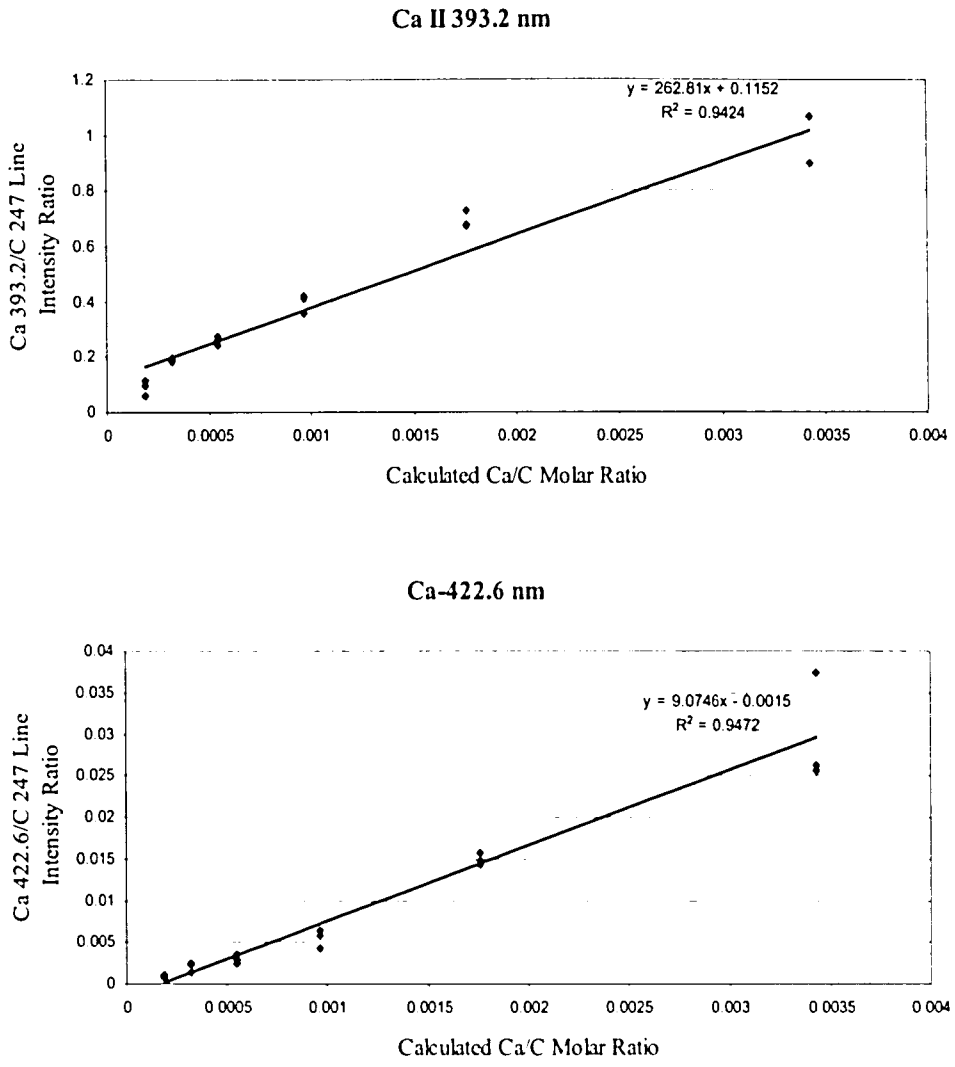

Figure 5.6: Calibration Plots for Ca Emission Lines

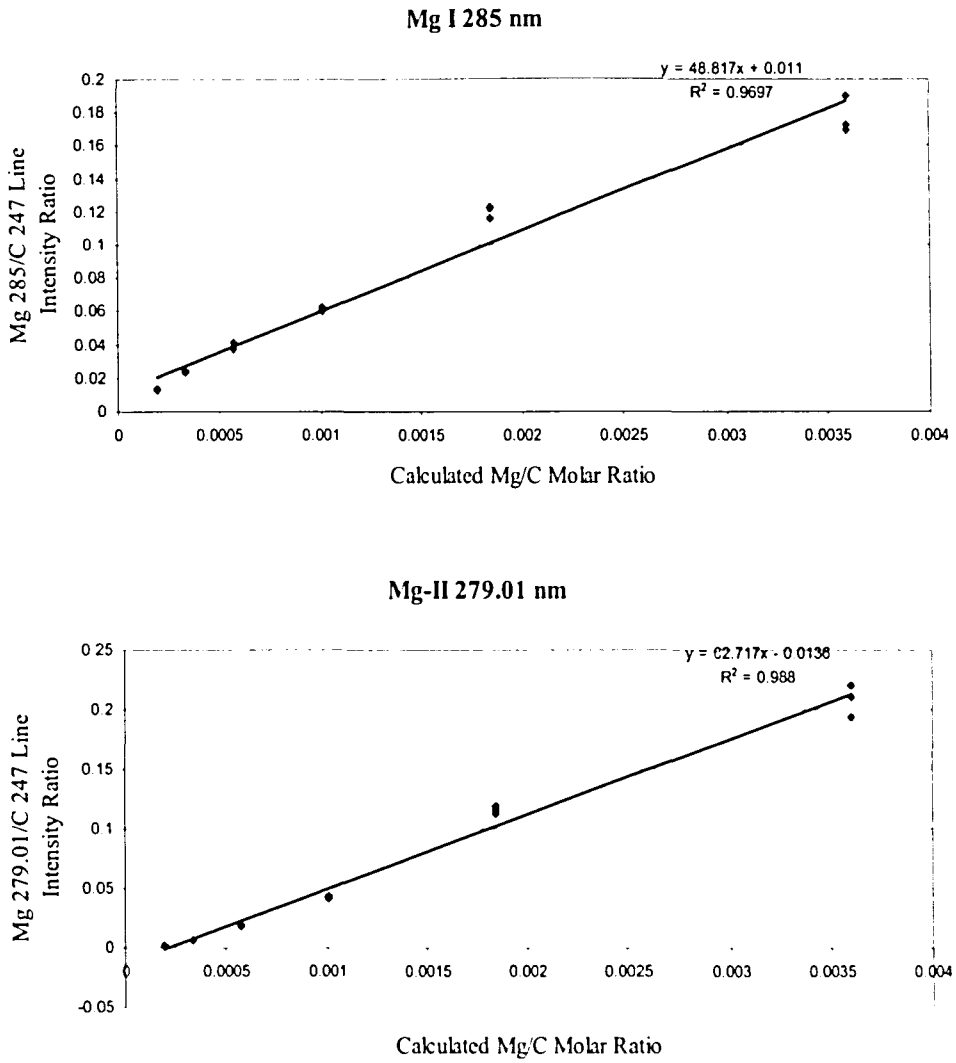

Figure 5.7: Calibration Plots for Mg Emission Lines

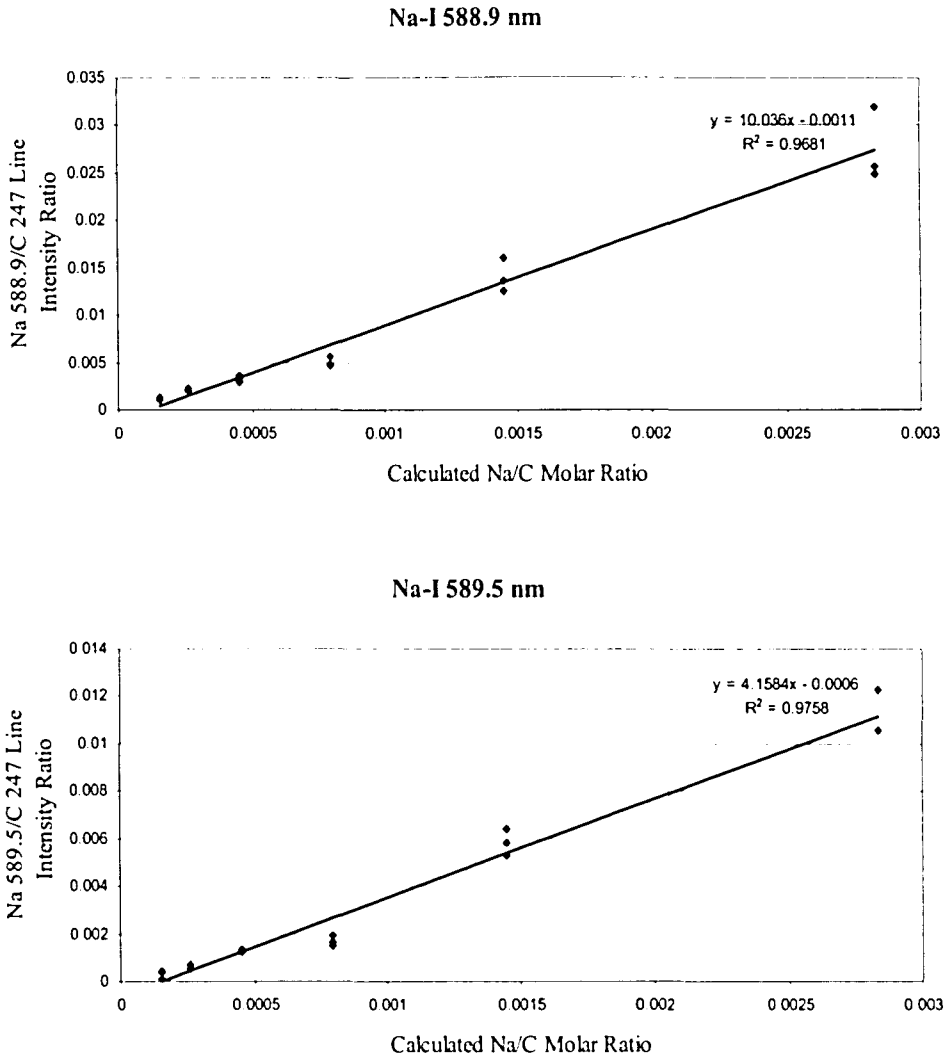

Figure 5.8: Calibration Plots for Na Emission Lines

K

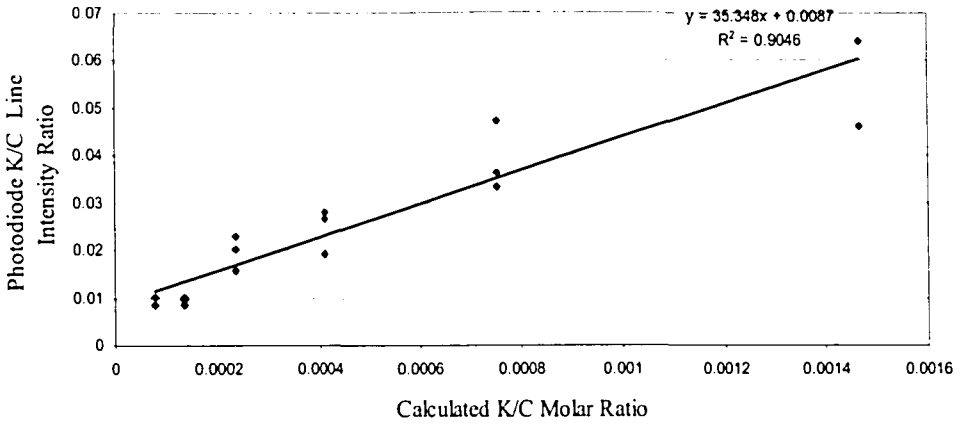

Figure 5.9: Calibration Plot for K Emission Line

O

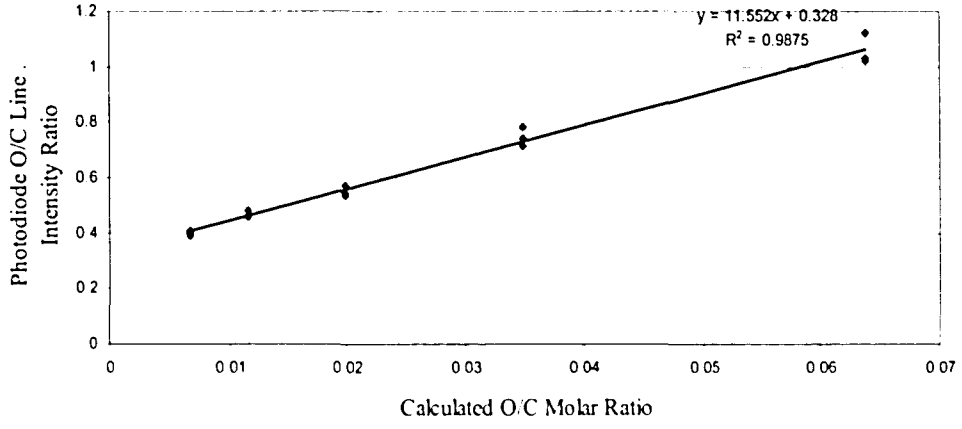

Figure 5.10: Calibration Plot for O Emission Line

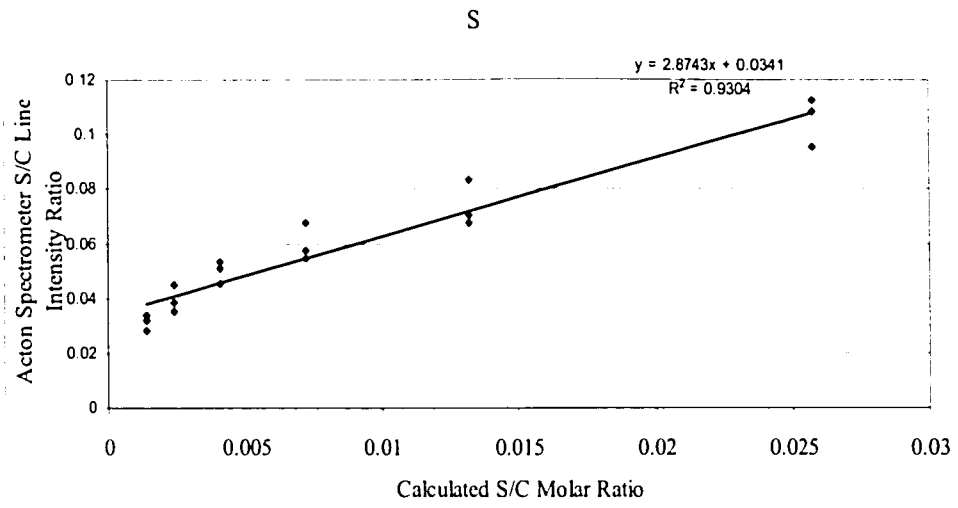

Figure 5.11: Calibration Plot for S Emission Line

In Figures 5.2 to 5.11, a trend line was added in each plot and the R-square values were calculated. R-square is a parameter used in regression analysis. Regression is a technique of fitting a simple equation to real data points. The most typical type of regression is the linear regression, constructed using the least-squares method (see Figure 5.11). It is customary to use a formula of the form: $y = bx + a$

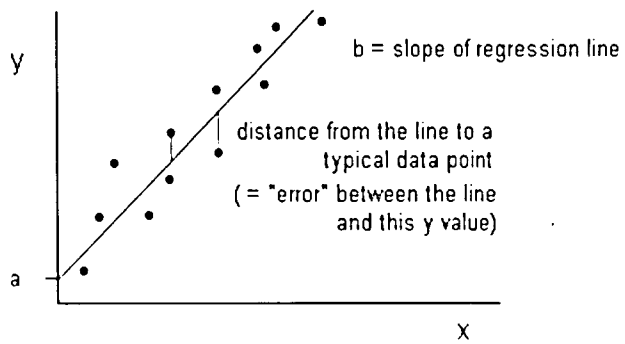

Figure 5.12 Linear Regression Example Plot

R-Square is a statistical measure of how well a regression line approximates real data points. An R-square of 1.0 (100 percent) indicates a perfect fit. Mathematically, the standard deviation is a statistical measure of the distance a quantity is likely to lie from its average value, and it is defined as:

$$StdDev(r) = [1/n * \Sigma (r_i - r_{ave})^2]^{1/2} \quad (5.11)$$

In this study, in Figure 5.2 to Figure 5.10, plots with an R-square value greater than 0.8 were considered to have good linear correlations. According to the R-square values in the plots, all the R-squares for the different elements in the simulated coals resulted to be over 0.9, therefore, indicating a good correspondence and reproducibility of the molar ratio to carbon from the LIBS measurements.

5.2 Experimental Results for Coal Samples

Based on the results obtained from the synthetic coal samples, LIBS experiments were performed using a set of coal samples assembled for this study. The coal bank consisted of 19 samples, encompassing a range of slagging propensities. The 19 coal samples were collected from different coal-fired power plants with whom the Lehigh University Energy Research Center has a working relation and it are reported to have slagging issues of some sort. A full set of standardized ASTM analysis (ASTM Methods D5142-04, D3176-89, D3682-01, etc.), was performed on these samples to obtain proximate analysis, ultimate analysis, mineral analysis and fusion temperature

analysis data. These analysis results were then used to calculate slagging indicators, Fs and Ti for these coals. In the Table 5.3, the analysis results for the coals in the coal collection are shown. The Table 5.3 also includes all the chemical property values, calculated slagging and fouling indices and the indices performance ranges.

With the results obtained from the LIBS tests on the simulated coal samples, LIBS experiments can be performed on the coal samples especially collected for this study. For the LIBS tests for the collected 19 coals samples, the same experimental settings were applied as in the tests for the simulated samples. Four tests for each coal were performed and LIBS data were collected and processed. Samples prepared for each test were well ground into fine powders, and handled with a rifler to be evenly divided into four equal parts. These fours parts were treated as four different samples and tested separately, the data from those four LIBS tests were collected and processed separately too. This procedure was taken to reduce the influence from the unevenly distributions of the elements concentrations in the coal sample. Seventy-six tests were taken for the 19 coal samples. In each test, coal powder was placed on a double layer sticky tape in the LIBS test plate, and fed into the chamber for testing. The chamber was filled with helium gas and chamber pressure was maintained at 21 inches Hg during the test. 100 laser shots were taken for each sample, and LIBS data were collected and processed by the spectrometers and computers, the final data used were averaged from 100 shots.

The processed data from the LIBS experiments from the 19 coals sample were

compared to the chemical analysis provided for the coal samples. The final objective would be to use reproducible LIBS coal elemental data into the neurofuzzy and mathematical methods already developed for Fs and Ti to build slagging predicting models. The LIBS-generated data for each element of interest consisted of intensity data at specific wavelengths. Intensity of at least 500 counts was used to distinguish peaks from the base noise (normally less than 100 counts). The results for all coals and all elements were proved to be inconsistent. However, some coals and some elements showed a consistent correlation between the concentration determined with the LIBS technique and the concentration reported from the standardized analysis accompanying the particular coal. An error calculation similar to the one performed for the simulated coal experiments was performed for those elements where good reproducibility was achieved by the LIBS technology. Error values less than 0.3 were considered as good. Figures 5.13 to 5.19 show comparative plots for the following species that were reproduced by the LIBS technique: Al, Ca, Fe, Mg, Na, Si and Ti.

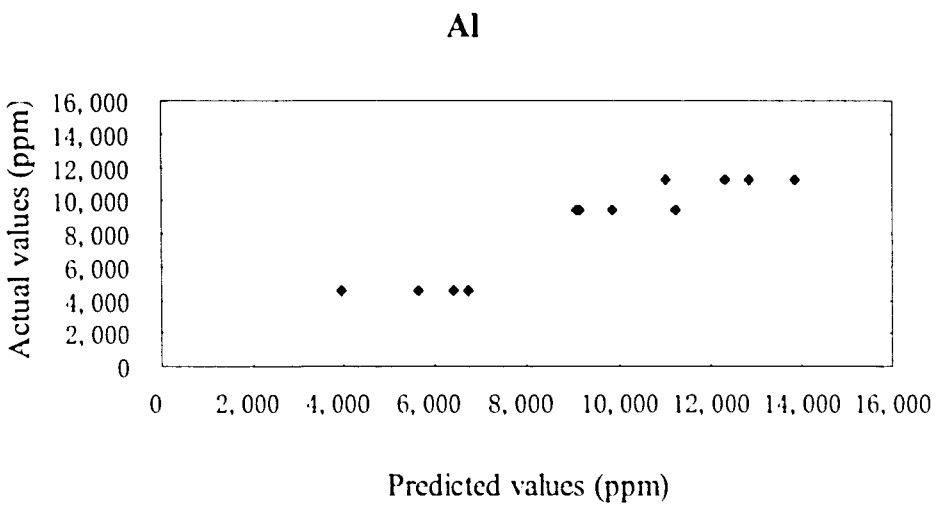

Figure 5.13: Predicted Al Element Concentration VS. the Actual Al Element Concentration. Error Function x_{Al}=0.169

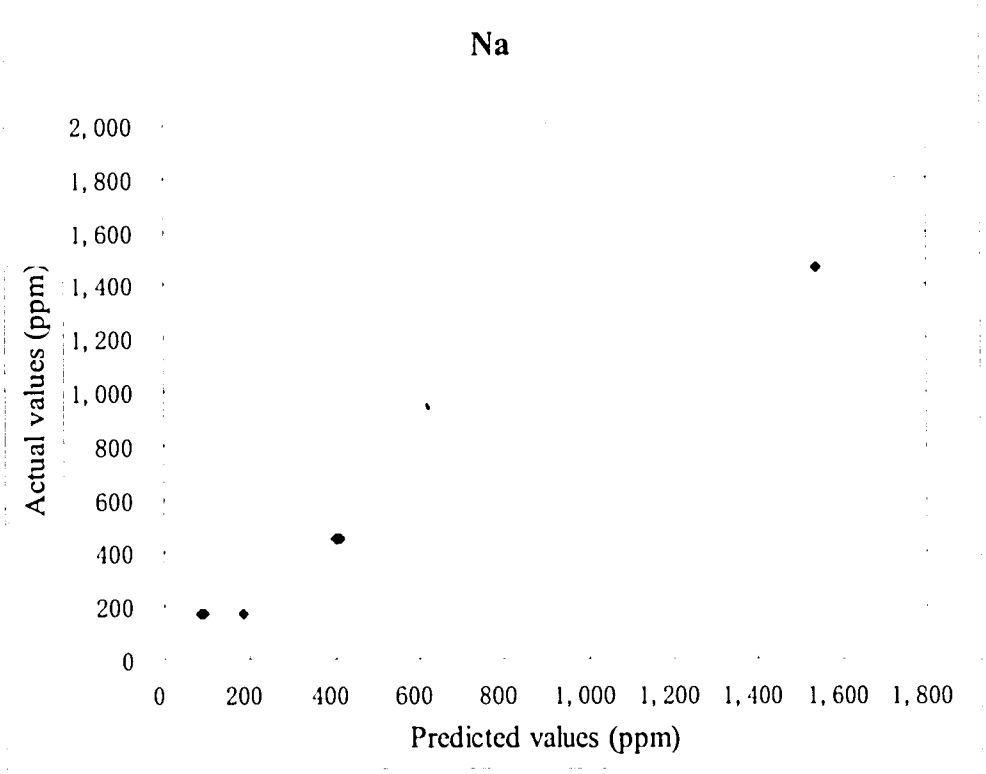

Figure 5.14: Predicted Na Element Concentration VS. the Actual Na Element Concentration. Error Function x_{Na}=0.174

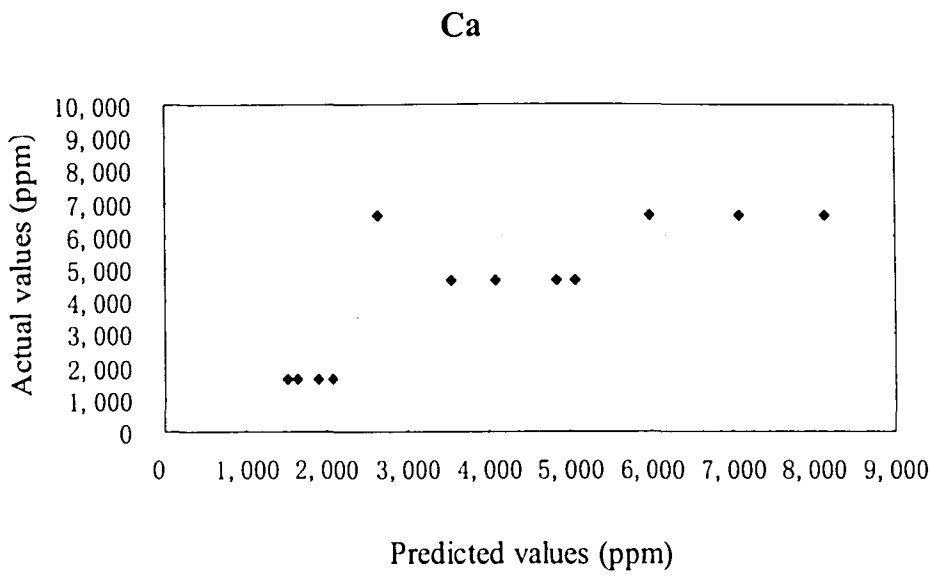

Figure 5.15: Predicted Ca Element Concentration VS. the Actual Ca Element Concentration. Error Function x_{Ca} =0.167

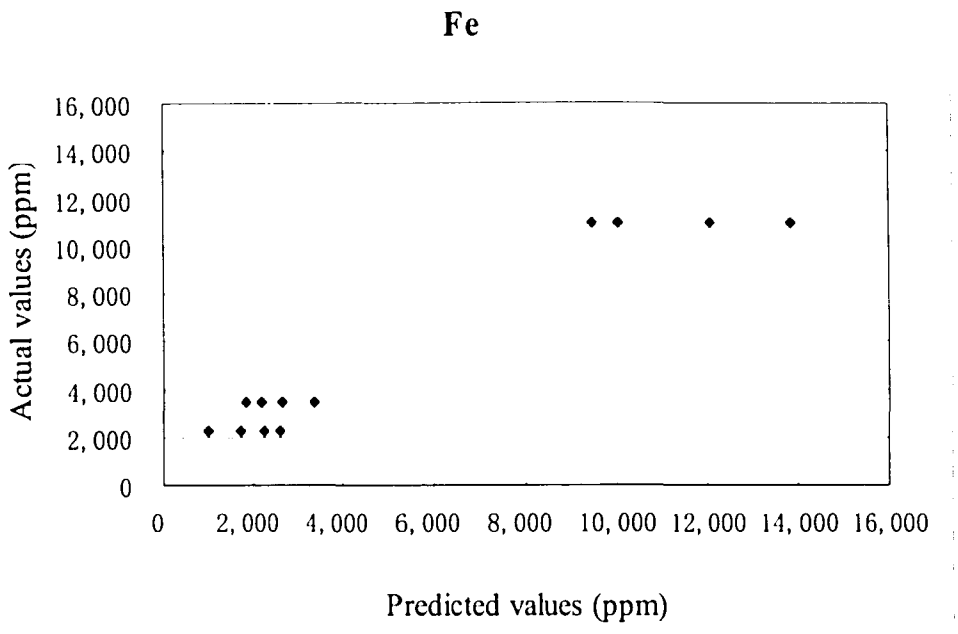

Figure 5.16: Predicted Fe Element Concentration VS. the Actual Fe Element Concentration. Error Function x_{Fe}=0.225

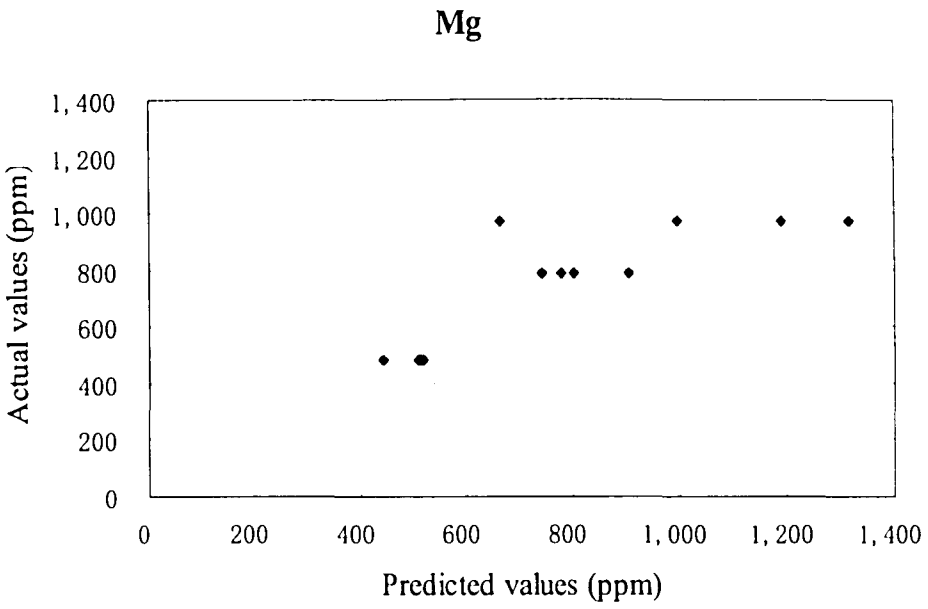

Figure 5.17: Predicted Mg Element Concentration VS. the Actual Mg Element Concentration. Error Function x_{Mg} =0.121

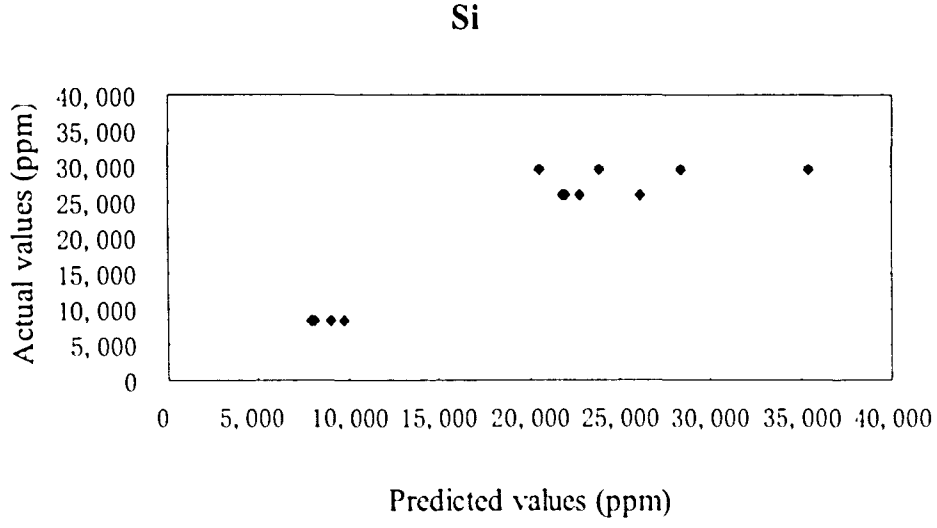

Figure 5.18: Predicted Si Element Concentration VS. the Actual Si Element Concentration. Error Function x_{Si}=0.122

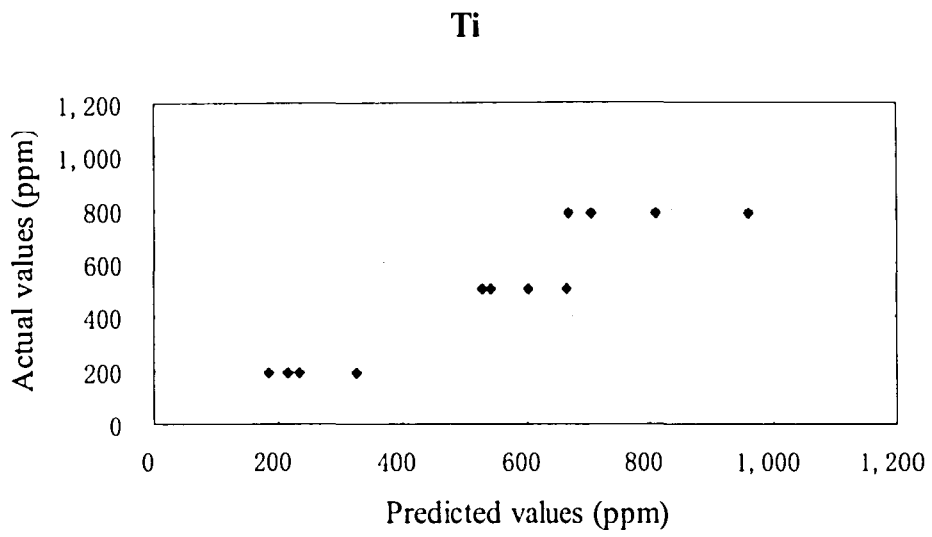

Figure 5.19: Predicted Ti Element Concentration VS. the Actual Ti Element Concentration. Error Function x_{Ti}=0.189

The elements Al, Ca, Fe, Mg, Si, Na and Ti, for which the experimental error was less than 0.3 were estimated from data collected by the Echelle spectrometer. It is apparent that due to the deficiencies in the resolution of the other detection elements in the LIBS system, measurement of K and S (which were collected by the Acton spectrometer and the photodiodes), did not generate consistent and reproducible data to build for slagging model building. Hence, the resolution for the Acton spectrometer and the photodiode array need some improvement to correctly collect accurate K and S LIBS signatures. These two parameters are both involved as important parameters in the slagging predictors Fs and Ti.

Chapter 6: Conclusions and Recommendations

6.1 Conclusions

LIBS is a technology which uses a laser to excite atoms from a sample and then collects and processes the emission light data to quantify the components of the tested samples. The LIBS technology has been widely applied in different research areas. In this study, the LIBS technology was introduced to a coal-fired power plant application for the prediction coal slagging propensity. A group of slagging indices were searched and analyzed, and two slagging indices: base to acid ratio times dry sulfur "Fs" and ash fusion temperature "Ti" were selected as indicators of coal slagging propensity. Models were developed and tested using data from the US Geological coal database. One model is an artificial intelligence neurofuzzy model chosen to predict Fs. The other model is a non-linear mathematical function chosen to predict Ti.

LIBS experiments were performed on simulated mixture samples, simulating the ratio of the element of interest (for the developed models) to carbon. A comparison of the performance of the LIBS technology to reproduce the analytical concentration of these simulated coal compounds indicate that the LIBS technique was successful in reproducing the simulated concentrations with R-square better than 0.8. Afterwards, LIBS tests were performed on 19 coals collected by the Energy Research Center. The results of the LIBS experiments of real coal samples were less encouraging, with good accuracy for the detection of Al, Ca, Fe, Mg, Si, Na and Ti (detected by the Echelle spectrometer), and less accuracy in the prediction of K and S, which most likely due to

the lack of resolution on the part of the Acton spectrometer and the photodiode array.

There appears to be good potential for researchers to make future developments in the energy area using the LIBS technology. Due to the small dimensions of the LIBS technique, it may be possible to develop an integrated compact instrument for field use which contains all the components of the LIBS laboratory system. With a small, portable instrument installed in power plants, coal chemical analysis could be accomplished by the LIBS technology in-situ and in real-time.

6.2 Recommendations

The LIBS technology is still in its starting stages, and it can possibly be improved in many ways. Due to the lack of current instrument resolutions, LIBS measurements for a few elements were not consistent. Thus, the LIBS experimental system should be improved by increasing the resolutions of the photodiode and spectrometers before more integrated results can be obtained. The following specific recommendations are made:

- Due to the limitations of the current experimental equipment, the LIBS signals for some of the elements from the Acton spectrometer and photodiodes were not quite good. In order to perform prediction of the slagging indices, Fs and Ti, nine selected elements are needed from the LIBS systems on an accurate basis. Therefore, further work on this subject should focus on improving the resolutions of the spectrometers.

- It would be helpful for prediction results to build up a broader coal database by expanding the 19-coals coal bank used in the study. These coals should be well studied on their slagging properties from long term field use, as well as tested in the laboratory so that the actual concentrations of related elements are known. Also, since the major coal types of current 19 coals are bituminous and sub-bituminous coals, more supplementary coals under these two categories and other coal ranks should be added. Besides, coals with extended variations in the ranges of metals and other elements should be considered.

- The LIBS technology can be further developed and introduced to the field of coal properties detection. For example, a compact LIBS detector could possibly be developed and installed in a power plant or other similar environment. By using the LIBS technology, a lot of time and expense can be saved compared to laboratory analysis. In addition, slagging phenomena happening inside the boilers can be inferred through the use of a LIBS detector.

Reference

[1.1] Yong-Ill Lee, Kyuseok Song and Joseph Sneddon (2000) *Laser-Induced Breakdown Spectrometry,* Huntington, NY: Nova Science Publishers

[2.1] Steven A. Benson (2001) *Predicting Ash Formation and Behavior,* http://www.microbeam.com/PDF%20Articles/Predicting%20Ash%20Formation%20and%20Behavior.pdf (view date: 04/15/2007)

[2.2] Gordon Couch (1994) *Understanding Slagging And Fouling In Pf Combustion*, IEA Coal Report, IEA Research, London

[2.3]. Attig, R. C. and Duzy, A. F.(1969) *Coal Ash Depositional Studies And Application To Boiler Design* in American Power Conference, Illinois Institute of Technology, Chicago, IL

[2.4]. Winegartner, E. C. (ed.) (1974), *Coal Fouling and Slagging Parameters*, ASME research Committee on Corrosion and Deposits from Combustion Gases, ASME pub.

[2.5] Rod Hatt (1995) *Correlating The Slagging Of A Utility Boiler With Coal Characteristics* in Engineering Foundation Conference, Waterville Valley, NH

[2.6]. Robert R. Jensen, Steven A. Benson, Jason D. Laumb(2001) *Subtask 3.6 - Advanced Power Systems Analysis Tools*, Final Report, U.S. Department of Energy, National Energy Technology Laboratory

[2.7] Maria Mastalerz, Agnieszka Drobniak, John Rupp, and Nelson Shaffer (2004) *Characterization of Indiana's Coal Resource: Availability of the Reserves, Physical and Chemical Properties of the Coal, and the Present and Potential Uses*, Final Report To The Center For Coal Technology, Indiana University, Bloomington, IN

[2.8] Ottesen, DK; Baxter, LL; Radziemski, LJ; Burrows, JF (1991) *Laser Spark*

Emission Spectroscopy For In Situ, Real-Time Monitoring Of Pulverized Coal Particle Composition Energy & Fuels In: Energy Fuels, Vol. 5, no. 2, pp. 304-312,

[2.9] Miki Kurihara, Koji Ikeda, Yoshinori Izawa, Yoshihiro Deguchi, and Hitoshi Tarui (2003) *Optimal Boiler Control Through Real-Time Monitoring Of Unburned Carbon In Fly Ash By Laser-Induced Breakdown Spectroscopy* In: Applied Optics, Vol. 42, No. 30

[2.10] Wallis, Fiona J.; Chadwick, Bruce L.; Morrison, Richard J.S. (2000) *Analysis of Lignite Using Laser-Induced Breakdown Spectroscopy* In: Applied Spectroscopy, Vol. 54, No. 8, pp. 1231-1235(5), Society for Applied Spectroscopy

[2.11] Doug Body and Bruce L. Chadwick (2001) *Simultaneous Elemental Analysis System Using Laser Induced Breakdown Spectroscopy* In: Review Of Scientific Instruments Vol. 72, No. 3, American Institute of Physics

[2.12]. Linda G. Blevins, Christopher R. Shaddix, Shane M. Sickafoose, and Peter M. Walsh (2003) *Laser-Induced Breakdown Spectroscopy at High Temperatures in Industrial Boilers And Furnaces* In: Applied Optics, Vol. 42, No. 30, 20

[2.13] Yu Liangying, Shen Kai, Feng Wei, L U Jidong, Chen Wen, Wu Ge (2005) *Analysis of Pulverized Coal by Laser-Induced Breakdown Spectroscopy* In: Plasma Science & Technology, Vol.7, No.5, China

[2.14] M. Noda, Y. Deguchi, S. Iwasaki, N. Yoshikawa (2002) *Detection Of Carbon Content In A High-Temperature And High Pressure Environment Using Laser-Induced Breakdown Spectroscopy*, In: Spectrochimica Acta, Part B: Atomic Spectroscopy, Volume 57, Number 4, 5, Elsevier, pp. 701-709(9)

[2.15] Zhang, Hansheng; Singh, Jagdish P; Yueh, Fang-Yu; Cook, Robert L. (1995) *Laser-Induced Breakdown Spectra in a Coal-Fired MHD Facility* In: Applied

Spectroscopy, Vol. 49, No. 11, pp.1617-1623(7)

[4.1] *Neuframe v.4*, Neusciences, Totton, Southampton, UK

[4.2] U.S. Geological Survey, *U.S. Geological Coal Database,*

http://energy.er.usgs.gov/coalqual.htm (view date: 04/15/2007)

[5.1] Jim Simpson (2007) *Summary of Simulated Coal Results*, Energy Research Co., State Island, NY

Vita

Yao Shen

Birth Date: July 28th, 1981

Birth Place: Shenyang, China

Name of Parents: Liying Shen(Father), Hongjian Ding(Mother)

Institutes Attended and Degrees:

Lehigh University, Bethlehem, USA

Master of Science in Mechanical Engineering (to be awarded) 05/2007

Peking University, Beijing, China

Bachelor of Science in Mechanical Engineering 06/2004

Research Area: Energy Research in Mechanical Engineering

Professional Experiences:

Research Assistant 05/2005-07/2006
Energy Research Center, Lehigh University, Bethlehem, Pennsylvania
Laboratory and field research on the boiler system and other energy-related topics.

END OF TITLE